PHYSICAL REVIEW D **92,** 115018 (2015)

Vectorlike leptons at the Large Hadron Collider

Nilanjana Kumar[1] and Stephen P. Martin[1,2]

[1]*Department of Physics, Northern Illinois University, DeKalb, Illinois 60115, USA*
[2]*Fermi National Accelerator Laboratory, P.O. Box 500, Batavia, Illinois 60510, USA*

(Received 26 October 2015; published 22 December 2015)

We study the prospects for excluding or discovering vectorlike leptons using multilepton events at the LHC. We consider models in which the vectorlike leptons decay to tau leptons. If the vectorlike leptons are weak isosinglets, then discovery in multilepton states is found to be extremely challenging. For the case that the vectorlike leptons are weak isodoublet, we argue that there may be an opportunity for exclusion for masses up to about 275 GeV by direct searches with existing LHC data at $\sqrt{s} = 8$ TeV. We also discuss prospects for exclusion or discovery at the LHC with future $\sqrt{s} = 13$ TeV data.

DOI: 10.1103/PhysRevD.92.115018 PACS numbers: 12.60.-i

I. INTRODUCTION

Vectorlike quarks and leptons are hypothetical new fermions that transform in nonchiral representations of the unbroken Standard Model (SM) gauge group. They are among the simplest viable SM extensions near the electroweak scale. Vectorlike fermions can have electroweak singlet masses that dominate over the contributions to their masses from Yukawa couplings to the Higgs boson. This means that their loop-induced contributions to precision electroweak observables and radiative Higgs decays and production obey decoupling with large masses. Therefore, vectorlike fermions are less constrained than extra chiral families, which are now ruled out by a combination of direct searches and the observations of the 125 GeV Higgs boson production and decay. In the absence of large lepton flavor violation, general mass limits on vectorlike fermions with nonexotic electric charges therefore follow only from direct searches.

Besides the mere fact that they are possible, there are a variety of motivations to consider vectorlike fermions. From a top-down perspective, phenomenological models motivated by string theory or large extra dimensions are well known to be often replete with such particles. In weak-scale supersymmetry, the mass of the lightest Higgs scalar boson can be raised by introducing new vectorlike heavy chiral supermultiplets with large Yukawa couplings [1–15]. The correction to M_h is positive if the vectorlike fermions are lighter than their scalar partners, which implies that the former could be the first physics beyond the SM to be detected at the Large Hadron Collider (LHC). Some other interesting discussions of the possible role of vectorlike leptons in physics beyond the SM are given in Refs. [16–45]. For vectorlike leptons with large exotic charges, there is also a possibility of indirect searches from the loop-induced process $pp \to pp\gamma\gamma$ [46].

In this paper we consider the LHC exclusion and discovery reach for vectorlike leptons in two scenarios. First, we consider $SU(2)_L$-singlet charged vectorlike leptons $\tau'^{\pm}$ which under $SU(3)_C \times SU(2)_L \times U(1)_Y$ transform as 2-component left-handed fermions[1]

$$\tau' + \bar{\tau}' = (\mathbf{1}, \mathbf{1}, +1) + (\mathbf{1}, \mathbf{1}, -1). \tag{1.1}$$

The second scenario consists of pure $SU(2)_L$-doublet particles $L' = (\nu', \tau'^{-})$ and their antiparticles $\bar{L}' = (\tau'^{+}, \bar{\nu}')$, which transform under $SU(3)_C \times SU(2)_L \times U(1)_Y$ as 2-component left-handed fermions

$$L' + \bar{L}' = (\mathbf{1}, \mathbf{2}, -1/2) + (\mathbf{1}, \mathbf{2}, +1/2). \tag{1.2}$$

In the following, we will refer to these as the singlet VLL and doublet VLL models, respectively. For simplicity, we consider these two possibilities separately, although models in which they are combined or replicated are certainly feasible, and would have a richer phenomenology.

The main source of vectorlike lepton masses are weak singlet terms. If these were the only sources of vectorlike lepton mass, then in the singlet VLL model the τ' would be absolutely stable, causing possible problems due to its presence as a charged exotic stable relic in the Universe. In the doublet VLL model the ν' would be stable. We will therefore assume that the vectorlike leptons mix through Yukawa interactions with the ordinary known leptons of the SM, allowing them to have 2-body decays to SM leptons and bosons W, Z, h, as described in more detail in the next section. Our premise, motivated by the relative weakness of lepton flavor-violation constraints involving the τ lepton compared to the electron and muon, is that the vectorlike lepton coupling to SM leptons is mostly with the third family, and therefore the τ' and ν' decay mostly to final states involving the τ lepton and Standard Model neutrinos. This is the most pessimistic possibility for LHC reach, due to the relatively lower detection efficiency and higher fake

[1]For reviews of the 2-component fermion notation followed here, see Refs. [47,48].

rates for τ candidates in the LHC detectors. An earlier study [40] instead considered the more optimistic possibility that vectorlike leptons produced at the LHC will decay mostly to muons. At this writing, there do not appear to be any official limits on vectorlike leptons from the LHC detector collaborations, so that the only constraint comes from the nondiscovery by the LEP e^+e^- collider experiments, of about $M_{\tau'} > 100$ GeV. In the following, we will consider the possibilities of setting limits on vectorlike leptons that decay to τ and Standard Model neutrinos using existing ATLAS multilepton searches, and using our own alternative search criteria, for pp collisions at $\sqrt{s} = 8$ TeV with 20 fb^{-1} of integrated luminosity. We will then consider the projected exclusion and discovery reaches of the LHC in multilepton searches in future runs with $\sqrt{s} = 13$ TeV. In these 3-, 4-, and 5-lepton searches, we rely both on τ leptons that are detected as hadronic taus, τ_h, and on τ leptons that decay leptonically to electrons and muons.

In consideration of exclusion and discovery prospects, we will employ the following criteria. For a given hypothesis H_0, we estimate the median expected p-value p, which is the probability, for data generated under a hypothesis H, of observing a result of equal or greater incompatibility with H_0. As is conventional in high-energy physics, the p-value is converted to a significance Z according to

$$Z = \sqrt{2}\mathrm{erfc}^{-1}(2p). \tag{1.3}$$

In the case of a standard Gaussian distribution, Z corresponds to the number of standard deviations. In the case of discovery, H_0 is the background-only hypothesis of a Poisson distribution of events with mean b, while H is the hypothesis of a Poisson distribution of signal and background events with mean $s + b$. However, the background levels are not, and will not be, known with perfect accuracy. Therefore we include the effects of a variance Δ_b in the expected number of background events. An approximation (see Ref. [49], and also Refs. [50] and [51,52]) for the median expected discovery significance is then

$$Z_{\rm disc} = \left[2\left((s+b)\ln\left[\frac{(s+b)(b+\Delta_b^2)}{b^2+(s+b)\Delta_b^2}\right] - \frac{b^2}{\Delta_b^2}\ln\left[1+\frac{\Delta_b^2 s}{b(b+\Delta_b^2)}\right]\right)\right]^{1/2}. \tag{1.4}$$

In the special case that the background expectation is known perfectly, so that $\Delta_b = 0$, this reduces to

$$Z_{\rm disc} = \sqrt{2[(s+b)\ln(1+s/b) - s]}, \tag{1.5}$$

which would further reduce to $s/\sqrt{b}$ in the limit of large b. However, when b is small, $s/\sqrt{b}$ greatly overestimates the expected significance. For a discovery criterion, we use $Z_{\rm disc} > 5$, corresponding to a p-value range $p < 2.86 \times 10^{-7}$, and we will use Eq. (1.4) with the somewhat arbitrary choices $\Delta_b = 0.1b$, $0.2b$, and $0.5b$, corresponding to a 10%, 20%, and 50% uncertainty in the background.

For exclusion, the role of H_0 is played by the signal plus background hypothesis, and H is the background-only hypothesis. We then find, based on methods in Refs. [49,50], an estimate for the median expected exclusion significance:

$$Z_{\rm exc} = \left[2\left\{s - b\ln\left(\frac{b+s+x}{2b}\right) - \frac{b^2}{\Delta_b^2}\ln\left(\frac{b-s+x}{2b}\right)\right\} - (b+s-x)(1+b/\Delta_b^2)\right]^{1/2}, \tag{1.6}$$

where

$$x = \sqrt{(s+b)^2 - 4sb\Delta_b^2/(b+\Delta_b^2)}. \tag{1.7}$$

In the special case $\Delta_b = 0$, Eq. (1.6) reduces to

$$Z_{\rm exc} = \sqrt{2(s - b\ln(1+s/b))}, \tag{1.8}$$

which further reduces to $s/\sqrt{b}$ in the limit of large b. Again, for small b, the latter overestimates the expected exclusion significance. For a median expected 95% confidence level (C.L.) exclusion ($p = 0.05$), we will use Eq. (1.6) with $Z_{\rm exc} > 1.645$, and again consider $\Delta_b = 0.1b$, $0.2b$, and $0.5b$. In the case of the singlet VLL model only, where the signal is quite small, we will also consider the very optimistic case $\Delta_b = 0$.

II. PRODUCTION AND DECAY OF VECTORLIKE LEPTONS

In the singlet VLL model, the fermion mass terms and τ' mixing with the Standard Model lepton can be obtained from the Lagrangian written in 2-component fermion form as

$$-\mathcal{L} = m_{\tau'}\tau'\bar{\tau}' + \epsilon HL\bar{\tau}' + y_\tau HL\bar{\tau} + \text{c.c.} \tag{2.1}$$

where H is the SM Higgs complex doublet scalar field, $L = (\tau, \nu_\tau)$ is the SM third family lepton doublet in the gauge eigenstate basis, y_τ is the SM τ Yukawa coupling, and ϵ is the mixing Yukawa coupling. The charged fermion mass matrix in the gauge eigenstate basis is

$$-\mathcal{L} = \begin{pmatrix}\tau & \tau'\end{pmatrix}\mathcal{M}\begin{pmatrix}\bar{\tau}\\ \bar{\tau}'\end{pmatrix} + \text{c.c.}, \tag{2.2}$$

where

$$\mathcal{M} = \begin{pmatrix} y_\tau v & \epsilon v \\ 0 & m_{\tau'}\end{pmatrix}, \tag{2.3}$$

and $v = \langle H \rangle = 174$ GeV is the Higgs vacuum expectation value (VEV). For the doublet VLL model, the Lagrangian is

$$-\mathcal{L} = m_{\tau'} L' \bar{L}' + \epsilon H L' \bar{\tau} + y_\tau H L \bar{\tau} + \text{c.c.}, \quad (2.4)$$

so that the charged mass matrix is instead

$$\mathcal{M} = \begin{pmatrix} y_\tau v & 0 \\ \epsilon v & m_{\tau'} \end{pmatrix}. \quad (2.5)$$

In both cases, we will take the Yukawa coupling ϵ to be small. Then, neglecting effects suppressed by ϵ, the charged lepton mass eigenstates include just a τ' with mass $M_{\tau'} \approx m_{\tau'}$, and the SM tau lepton with mass $M_\tau \approx y_\tau v$.

In the doublet VLL model, there is also a ν' state, with mass degenerate with the τ' at tree level. Taking into account 1-loop radiative corrections [18] while still neglecting the effects quadratic in ϵ, there is a small mass splitting

$$M_{\nu'} = M_{\tau'} - \frac{\alpha}{2} M_Z f(M_{\tau'}^2/M_Z^2), \quad (2.6)$$

where [18]

$$f(r) = \frac{\sqrt{r}}{\pi} \int_0^1 dx (2-x) \ln(1 + x/r(1-x)^2) \quad (2.7)$$

is positive and approaches 1 from below as r becomes very large. For $M_{\tau'} = (100, 200, 300$ GeV, and $\infty)$, this mass splitting is respectively about (258, 297, 313, 355) MeV, and will be only very slightly increased by mixing, by approximately $\epsilon^2 v^2/2M_{\tau'}$. For kinematic purposes, we will therefore simply take $M_{\nu'} = M_{\tau'}$.

The production rates for vectorlike leptons are governed to a very good approximation by their lepton flavor-preserving interactions with the electroweak vector bosons. In 2-component fermion notation [with a metric signature $(-, +, +, +)$] in the mass eigenstate basis, the singlet VLL model has, neglecting terms quadratic in ϵ,

$$\mathcal{L}_{\text{int}} = \frac{g s_W^2}{c_W} Z_\mu (\tau'^\dagger \bar{\sigma}^\mu \tau' - \bar{\tau}'^\dagger \bar{\sigma}^\mu \bar{\tau}') - e A_\mu (\tau'^\dagger \bar{\sigma}^\mu \tau' - \bar{\tau}'^\dagger \bar{\sigma}^\mu \bar{\tau}'), \quad (2.8)$$

where e is the QED coupling, g is the $SU(2)_L$ coupling, and s_W, c_W are the sine and cosine of the weak mixing angle, with $e = g s_W$. For the doublet VLL model, the Lagrangian governing τ' and ν' production is similarly

$$\begin{aligned} \mathcal{L}_{\text{int}} = {} & \frac{g}{\sqrt{2}} W_\mu^+ (\bar{\tau}'^\dagger \bar{\sigma}^\mu \bar{\nu}' + \nu'^\dagger \bar{\sigma}^\mu \tau') \\ & + \frac{g}{\sqrt{2}} W_\mu^- (\tau'^\dagger \bar{\sigma}^\mu \nu' + \bar{\nu}'^\dagger \bar{\sigma}^\mu \bar{\tau}') - e A_\mu (\tau'^\dagger \bar{\sigma}^\mu \tau' - \bar{\tau}'^\dagger \bar{\sigma}^\mu \bar{\tau}') \\ & + \frac{g}{c_W} \left(s_W^2 - \frac{1}{2} \right) Z_\mu (\tau'^\dagger \bar{\sigma}^\mu \tau' - \bar{\tau}'^\dagger \bar{\sigma}^\mu \bar{\tau}') \\ & + \frac{g}{2 c_W} Z_\mu (\nu'^\dagger \bar{\sigma}^\mu \nu' - \bar{\nu}'^\dagger \bar{\sigma}^\mu \bar{\nu}'). \end{aligned} \quad (2.9)$$

In the singlet VLL model, the production channel at the LHC is

$$pp \to \tau'^+ \tau'^-, \quad (2.10)$$

through s-channel Z, γ, while in the doublet VLL model one has in addition the processes involving the heavy vectorlike Dirac neutrino:

$$pp \to \nu' \bar{\nu}', \quad (2.11)$$

$$pp \to \nu' \tau'^+, \quad (2.12)$$

$$pp \to \bar{\nu}' \tau'^-. \quad (2.13)$$

In both cases, the production rates are a function of only one free parameter, the mass $M_{\tau'}$. They are shown for $\sqrt{s} = 8$ and 13 TeV in Fig. 1 for the singlet VLL model and in Fig. 2 for the doublet VLL model. It is evident that the production cross sections are much larger in the doublet VLL model than in the singlet VLL model. This is partly because of the larger couplings, but also because τ' is accompanied by ν' in the doublet case.

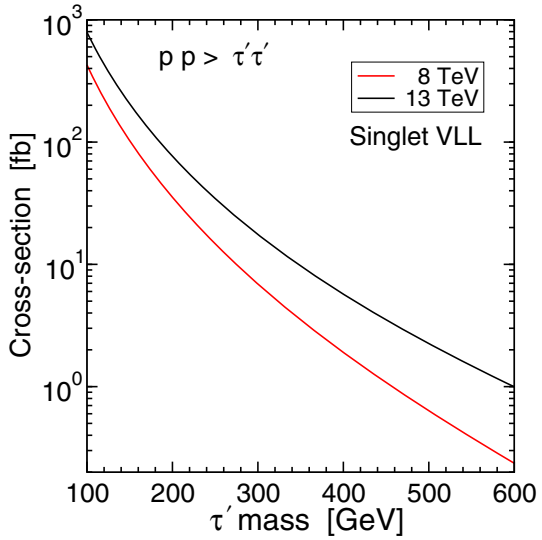

FIG. 1 (color online). The production cross section for $pp \to \tau'^+ \tau'^-$ as a function of the mass $M_{\tau'}$, for the LHC at $\sqrt{s} = 8$ and 13 TeV, in the singlet VLL model, mediated by the interactions in Eq. (2.8).

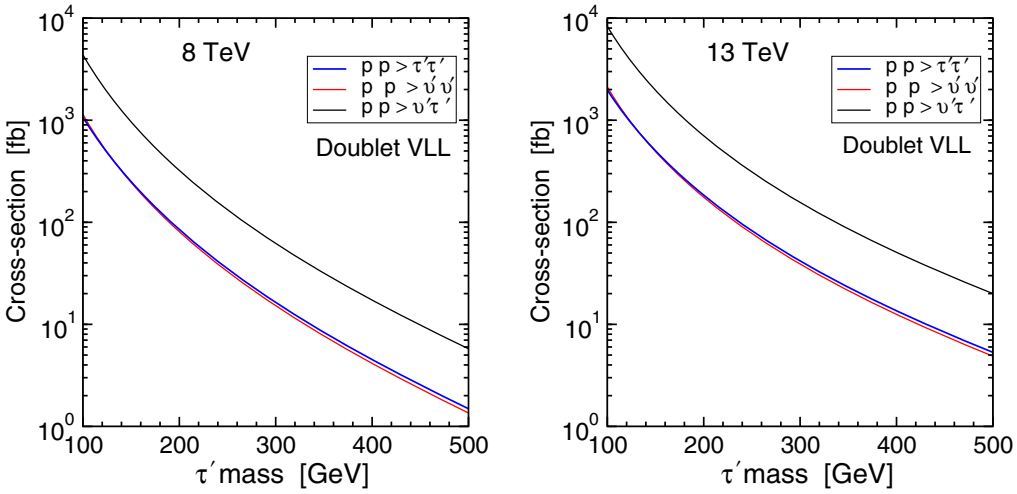

FIG. 2 (color online). The production cross sections for, from bottom to top, $\nu'\bar{\nu}'$ and $\tau'^{+}\tau'^{-}$ and the combined cross section for $\nu'\tau'^{+}$ and $\bar{\nu}'\tau'^{-}$, as a function of the common mass $M_{\tau'} = M_{\nu'}$, for the LHC at $\sqrt{s} = 8$ (left panel) and 13 TeV (right panel), in the doublet VLL model, mediated by the interactions in Eq. (2.9).

Indeed, the largest rate is from the $\nu'\tau'^{\pm}$ modes mediated by s-channel $W^{\pm}$ bosons. The LHC prospects for exclusion or discovery of the doublet VLL model are therefore much brighter than for the singlet VLL model, as we will see below.

We now turn to the interactions that mediate vectorlike lepton decays, which arise due to the mixing parameter ϵ. Working to linear order in ϵ, we have for the singlet VLL model

$$\begin{aligned}\mathcal{L}_{\rm int} = {} & g^{W^+}_{\nu^\dagger\tau'}[W^+_\mu(\nu^\dagger\bar{\sigma}^\mu\tau') + W^-_\mu(\tau'^\dagger\bar{\sigma}^\mu\nu)] \\ & + g^{Z}_{\tau^\dagger\tau'}Z_\mu(\tau^\dagger\bar{\sigma}^\mu\tau' + \tau'^\dagger\bar{\sigma}^\mu\tau) \\ & + (y^h_{\tau\bar{\tau}'}h\tau\bar{\tau}' + \text{c.c.}) \end{aligned} \tag{2.14}$$

where h is the real scalar field for the 125 GeV Higgs boson, and

$$g^{W^+}_{\nu^\dagger\tau'} = \epsilon M_W/M_{\tau'}, \tag{2.15}$$

$$g^{Z}_{\tau^\dagger\tau'} = -\epsilon M_Z/\sqrt{2}M_{\tau'}, \tag{2.16}$$

$$y^h_{\tau\bar{\tau}'} = -\epsilon/\sqrt{2}. \tag{2.17}$$

The resulting decay widths for τ' to SM states are

$$\Gamma(\tau' \to W\nu) = \frac{M_{\tau'}}{32\pi}(1-r_W)^2(2+1/r_W)|g^{W^+}_{\nu^\dagger\tau'}|^2, \tag{2.18}$$

$$\Gamma(\tau' \to Z\tau) = \frac{M_{\tau'}}{32\pi}(1-r_Z)^2(2+1/r_Z)|g^{Z}_{\tau^\dagger\tau'}|^2, \tag{2.19}$$

$$\Gamma(\tau' \to h\tau) = \frac{M_{\tau'}}{32\pi}(1-r_h)^2|y^h_{\tau\bar{\tau}'}|^2. \tag{2.20}$$

where $r_X = M_X^2/M_{\tau'}^2$ for $X = W, Z, h$.

For the doublet VLL model, the interactions that mediate decays of τ' and ν' are

$$\begin{aligned}\mathcal{L}_{\rm int} = {} & g^{W^+}_{\bar{\tau}^\dagger\bar{\nu}'}[W^+_\mu(\bar{\tau}^\dagger\bar{\sigma}^\mu\bar{\nu}') + W^-_\mu(\bar{\nu}'^\dagger\bar{\sigma}^\mu\bar{\tau})] \\ & + g^{Z}_{\bar{\tau}^\dagger\bar{\tau}'}Z_\mu(\bar{\tau}^\dagger\bar{\sigma}^\mu\bar{\tau}' + \bar{\tau}'^\dagger\bar{\sigma}^\mu\bar{\tau}) \\ & + (y^h_{\tau'\bar{\tau}}h\tau'\bar{\tau} + \text{c.c.}) \end{aligned} \tag{2.21}$$

where, again working to linear order in ϵ,

$$g^{W^+}_{\bar{\tau}^\dagger\bar{\nu}'} = -\epsilon M_W/M_{\tau'}, \tag{2.22}$$

$$g^{Z}_{\bar{\tau}^\dagger\bar{\tau}'} = -\epsilon M_Z/\sqrt{2}M_{\tau'}, \tag{2.23}$$

$$y^h_{\tau'\bar{\tau}} = -\epsilon/\sqrt{2}. \tag{2.24}$$

The resulting decay widths for τ' and ν' to SM states within this approximation are

$$\Gamma(\tau' \to W\nu) = 0, \tag{2.25}$$

$$\Gamma(\tau' \to Z\tau) = \frac{M_{\tau'}}{32\pi}(1-r_Z)^2(2+1/r_Z)|g^{Z}_{\bar{\tau}^\dagger\bar{\tau}'}|^2, \tag{2.26}$$

$$\Gamma(\tau' \to h\tau) = \frac{M_{\tau'}}{32\pi}(1-r_h)^2|y^h_{\tau'\bar{\tau}}|^2, \tag{2.27}$$

$$\Gamma(\nu' \to W\tau) = \frac{M_{\nu'}}{32\pi}(1-r_W)^2(2+1/r_W)|g^{W^+}_{\bar{\tau}^\dagger\bar{\nu}'}|^2, \tag{2.28}$$

$$\Gamma(\nu' \to Z\nu) = \Gamma(\nu' \to h\nu) = 0. \tag{2.29}$$

The resulting branching ratios only depend on the single parameter $M_{\tau'}$, as all of the widths are proportional to ϵ^2. These are shown in Fig. 3 for τ' in the singlet VLL model

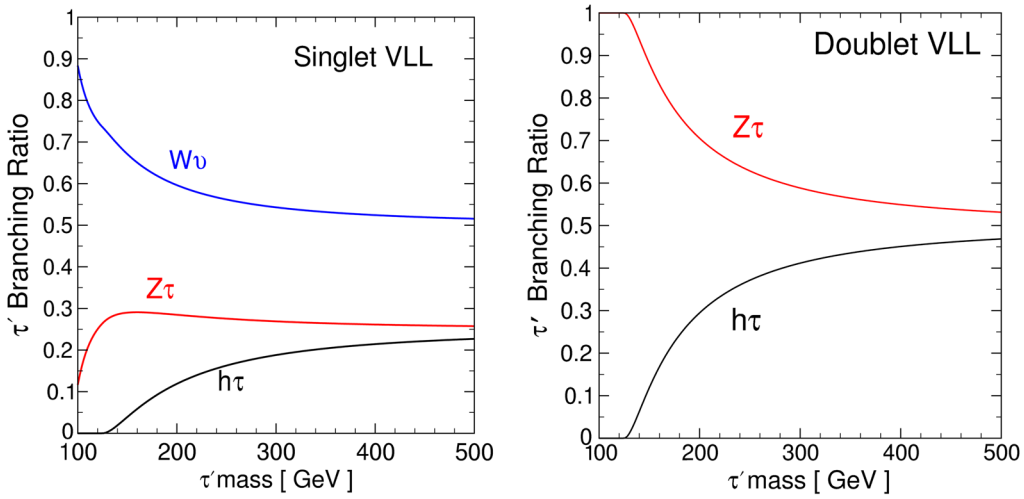

FIG. 3 (color online). The branching ratios for $\tau' \to W\nu$ and $Z\tau$ and $h\tau$, as a function of $M_{\tau'}$, for the singlet VLL model (left) and the doublet VLL model (right).

(left) and the doublet VLL model (right). Note that for $M_{\tau'} \gg M_h, M_Z, M_W$, the results asymptotically approach

$$\begin{aligned}&\mathrm{BR}(\tau' \to W\nu)\\ &:\mathrm{BR}(\tau' \to Z\tau):\mathrm{BR}(\tau' \to h\tau)\\ &\quad= \begin{cases} 2:1:1 & (\text{singlet VLL model}),\\ 0:1:1 & (\text{doublet VLL model}).\end{cases}\end{aligned} \tag{2.30}$$

Here, we have assumed that the highly kinematically suppressed decay of τ' to ν' is negligible. To justify this, note that from Ref. [18]

$$\Gamma(\tau' \to \nu'\pi^-) = (3.1 \times 10^{-14}\ \mathrm{GeV}) f^3 \sqrt{1 - 0.155/f^2}, \tag{2.31}$$

where $f = f(M_{\tau'}^2/M_Z^2)$ from Eq. (2.7). This decay width will be smaller provided that the dimensionless mixing Yukawa coupling satisfies $\epsilon \gtrsim 2 \times 10^{-7}$. This is also very roughly the condition needed for the decays of τ' and ν' to have a decay length $c\tau$ less than the centimeter scale, with some dependence of course on the mass. The doublet VLL model has

$$\mathrm{BR}(\nu' \to W^+\tau^-) = \mathrm{BR}(\bar{\nu}' \to W^-\tau^+) = 1. \tag{2.32}$$

This reflects our assumption of no mass mixing between ν' and the SM neutrinos. The large branching ratio of ν' into states with taus and possible leptons from the W decay helps the doublet VLL model exclusion and discovery prospects.

III. EVENT SIMULATION

From the results of the preceding section, we find the following signals for the singlet VLL model from τ' pair production Eq. (2.10):

$$ZZ\tau^+\tau^-, \qquad Zh\tau^+\tau^-, \qquad hh\tau^+\tau^-, \tag{3.1}$$

$$ZW^\pm\tau^\mp + E_T^{\mathrm{miss}}, \qquad hW^\pm\tau^\mp + E_T^{\mathrm{miss}}, \qquad W^+W^- + E_T^{\mathrm{miss}}, \tag{3.2}$$

while only the first 3 are produced by τ' pair production in the doublet VLL model. However, the doublet VLL model also has signals

$$W^+W^-\tau^+\tau^- \tag{3.3}$$

from ν' pair production Eq. (2.11), and

$$ZW^\pm\tau^+\tau^- \tag{3.4}$$

$$hW^\pm\tau^+\tau^- \tag{3.5}$$

from $\tau'\nu'$ production Eq. (2.12) and Eq. (2.13). In this paper, we consider final states with three or more leptons (including electrons and muons from leptonic tau decays, as well as hadronic taus, τ_h) that arise from these. This includes leptons coming from Higgs decays directly to taus and to W boson pairs, for which we use $M_h = 125$ GeV and the branching ratios

$$\mathrm{BR}(h \to \tau^+\tau^-) = 0.0605, \tag{3.6}$$

$$\mathrm{BR}(h \to W^+W^-) = 0.21. \tag{3.7}$$

In our signals, we often distinguish events depending on whether two opposite sign same flavor (OSSF) leptons reconstruct a Z boson.

For both the singlet and doublet VLL models, we have implemented the production and decay of τ' and ν' and their antiparticles in Madgraph 5 [53], which was used to generate both signal and background events. The couplings of the vectorlike leptons were discussed above. These couplings are included in the model files of FeynRules [54] to calculate the Feynman rules for the implementation into Madgraph. PYTHIA [55] was used for showering and hadronization. In order to do the detector simulation we used Delphes 3 [56]. In some cases below we found it useful to veto b jets in order to reduce backgrounds including $t\bar{t}Z$, $t\bar{t}W$ and $t\bar{t}h$. We chose the b-tagging efficiency for true b jets to be 0.7; the efficiency of mistagging a charm jet as b jet was 0.1, while for up, down and strange the mistagging efficiency was chosen to be 0.001. We have used the default Delphes tau tagging efficiency of 0.4, and tau misidentification rate for QCD jets is 0.001.

The main physics backgrounds for multilepton channels are WZ, ZZ, $t\bar{t}Z$, $t\bar{t}W$, hZ, $t\bar{t}h$, WWZ, ZZW, ZZZ, hh. They have also been simulated by Madgraph. We used K factors found from NLO and NNLO cross sections at 8 TeV from [57–60]. At 8 TeV the K factors are 1.58, 1.47, 1.38, 1.58, 1.315, 1.44, 1.8, 1.59, 1.591 following the same order of backgrounds as above excluding hh. Production of hh background includes the triangular and the box diagram. But the box diagram is not include in the Madgraph "heft" model package, so we generated events for hh using "heft" but we took the cross section for hh production from [61]. We took the same K factors to approximate the cross sections at 13 TeV. Except for the SM Higgs boson (h), every other particle in the background processes was forced to decay leptonically (including to tau leptons) in order to increase the yield in the simulation. In the cases of h decays to WW, ZZ, $b\bar{b}$, $\tau^+\tau^-$, and gg, we modified the Madgraph couplings of h to ensure agreement of the branching ratios with the theoretical predictions from HDECAY [62] for $M_h = 125$ GeV. At each of $\sqrt{s} = 8$ and 13 TeV, we generated 100,000 events for each of the backgrounds except for hh where we generated 500,000 events. To be conservative, we did not include K factors for the signal processes. The K-factors for $SU(2)_L$ triplets was recently found [63] to be in the range of about 1.17 to 1.2 for $\sqrt{s} = 13$ TeV, and the results for singlets and doublets should be about the same.

In the following sections, our study is divided in the following manner. First we looked at existing $\sqrt{s} = 8$ TeV multilepton searches by ATLAS, which were originally aimed at supersymmetric models but are repurposed here for vectorlike leptons. Unfortunately, we find no sensitivity to the singlet VLL model here, so our analysis is confined to the doublet VLL model. We then propose more inclusive 4-lepton searches, which are studied for the doublet VLL model with $\sqrt{s} = 8$ TeV. Finally, we consider the prospects for 4-lepton and 5-lepton signals at $\sqrt{s} = 13$ TeV for both the doublet and singlet VLL models, as well as an optimistic variant of the singlet VLL model in which one arbitrarily takes $\mathrm{BR}(\tau' \to Z\tau) = 1$.

IV. ATLAS MULTILEPTON SEARCHES AT $\sqrt{s} = 8$ TeV

As discussed above, vectorlike lepton models have a good possibility to provide a beyond Standard Model signature when pair-produced at the LHC and multilepton final-state channels are considered. In the following section we study the doublet VLL model first at $\sqrt{s} = 8$ TeV. We find that there is an opportunity to set limits on this model by using existing ATLAS searches at LHC [64,65] on 3-lepton and 4-lepton channels at $\sqrt{s} = 8$ TeV with $\int L\,\mathrm{dt} = 20.3\ \mathrm{fb}^{-1}$. We looked at 3-lepton channels first, and compared the visible signal cross sections after cuts with the limits from [64]. Similarly, for the 4-lepton analysis we compared with limits from [65]. While studying the VLL doublet model we always refer to $M_{\tau'} = M_{\nu'}$ as $M_{\tau'}$. For our study, we generated 100,000 signal events at $\sqrt{s} = 8$ TeV, for each of $M_{\tau'} = 110$, 130, 150, 180, 200, 250, 300, 400, and 500 GeV.

A. Three-lepton searches for the doublet VLL model

In this section we consider a search strategy based on requiring at least three leptons, following the selection criteria used by the ATLAS search at $\sqrt{s} = 8$ TeV and $\int L\,\mathrm{dt} = 20.3\ \mathrm{fb}^{-1}$, described in [64]. Lepton candidates (e, μ, τ_h) are required to satisfy

$$p_T > 15\ \mathrm{GeV}, \tag{4.1}$$

$$|\eta| < 2.4, \tag{4.2}$$

$$\Delta R_{\ell,\ell'} > 0.1 \quad (\text{for each} \ell, \ell' = e, \mu, \tau_h). \tag{4.3}$$

$$\Delta R_{\ell j} > 0.3 \quad (\text{for each jet and} \ell = e, \mu, \tau_h). \tag{4.4}$$

Events are then selected with at least three leptons, with at least one electron or muon satisfying a p_T trigger requirement:

$$N(e, \mu, \tau_h) \geq 3, \tag{4.5}$$

$$p_T(e_1/\mu_1) > 26\ \mathrm{GeV}. \tag{4.6}$$

After this selection, events are classified into two channels. One is events with at least three electron or muon candidates, and the other is events with exactly two electrons or muons and at least one hadronic tau ($2e/\mu + \geq 1\tau_h$). Events are then further classified into three categories. The first category is events with at least one

TABLE I. Visible cross sections σ_v in the $\geq 3e/\mu$ channel that pass the on-Z, off-Z, and off-Z, no-OSSF selections, in the doublet VLL model at $\sqrt{s} = 8$ TeV. The last line shows the ATLAS limit obtained at $\sqrt{s} = 8$ TeV with $\int L\,dt = 20.3$ fb^{-1}, from [64].

$M_{\tau'}$ (GeV)	σ_v on-Z (fb)	σ_v off-Z OSSF (fb)	σ_v off-Z no-OSSF (fb)
110	18.54	2.25	1.18
130	15.40	3.27	1.62
150	11.50	2.76	1.67
180	6.49	1.92	1.27
200	4.50	1.65	1.10
250	2.00	1.02	0.56
300	0.96	0.57	0.32
400	0.26	0.21	0.11
500	0.08	0.08	0.04
ATLAS limit	31	2.5	0.89

TABLE II. Visible cross sections σ_v in the $2e/\mu+ \geq 1\tau_h$ channel that pass the on-Z, off-Z, and off-Z, no-OSSF selections, in the doublet VLL model at $\sqrt{s} = 8$ TeV. The last line shows the ATLAS limit obtained at $\sqrt{s} = 8$ TeV with $\int L\,dt = 20.3$ fb^{-1} from [64].

$M_{\tau'}$ (GeV)	σ_v on-Z (fb)	σ_v off-Z OSSF (fb)	σ_v off-Z no-OSSF (fb)
110	12.96	3.24	6.19
130	11.58	2.78	8.08
150	7.57	2.25	7.08
180	3.92	1.43	5.18
200	2.68	1.16	4.18
250	1.04	0.57	2.07
300	0.47	0.33	1.10
400	0.11	0.11	0.34
500	0.03	0.04	0.12
ATLAS limit	207	14.0	4.3

opposite sign same flavor pair of leptons with 2-body invariant mass within 20 GeV of the Z boson mass. This category is referred to as on-Z. The second category is events with an OSSF pair that does not satisfy the on-Z requirement, and this category is called off-Z OSSF. All the remaining events contribute to the last category which is off-Z no-OSSF. Tables I and II list the visible cross sections we find after cuts for the signals in each category, for the doublet VLL model with various $M_{\tau'}$, along with the corresponding ATLAS limits from [64].

From Tables I and II, we see that there are three categories in which the signal cross sections after cuts can exceed the ATLAS bounds for a range of $M_{\tau'}$. Those cases are $\geq 3e/\mu$ off-Z OSSF, and $\geq 3e/\mu$ off-Z no-OSSF, and $2e/\mu+ \geq 1\tau_h$ off-Z no-OSSF. The estimated visible cross sections and corresponding ATLAS limits for these cases are depicted graphically in Fig. 4. The best reaches seem to be in the off-Z no-OSSF channels, where our estimates for the visible signal cross section exceed the ATLAS limit for all masses up to about $M_{\tau'} = 200$ GeV for both $\geq 3e/\mu$ and $2e/\mu+ \geq 1\tau_h$, where we expect more than about 22 and 84 signal events, respectively. It must be kept in mind that our studies based on Madgraph, PYTHIA and Delphes are certainly only an approximation to the real ATLAS (or CMS) experimental responses to signal events. We have not attempted to perform a detailed validation of our estimates in this case, as a true exclusion can only be established by the experimental collaborations in any case. Nevertheless, we can conclude from this study that using the 3-lepton channels, there is at least a possibility to set a limit on vectorlike lepton production in the doublet VLL model using existing LHC Run 1 data at $\sqrt{s} = 8$ TeV data.

B. Four-lepton searches for the doublet VLL model

In this section we consider 4-lepton signals for the doublet VLL model at $\sqrt{s} = 8$ TeV, this time using the selection criteria of the ATLAS search reported in Ref. [65]. Lepton candidates are required to satisfy

$$p_T(e,\mu) > 10 \text{ GeV}, \tag{4.7}$$

$$p_T(\tau_h) > 20 \text{ GeV}, \tag{4.8}$$

along with the same pseudorapidity and isolation requirements of Eqs. (4.2) and (4.4) above. Events are then required to have at least 4 leptons, of which at least 2 must be e, μ:

$$N(e,\mu,\tau_h) \geq 4, \tag{4.9}$$

$$N(e,\mu) \geq 2, \tag{4.10}$$

and to pass through at least one of the following four trigger criteria:

(i) $p_T(e_1/\mu_1) > 25$ GeV for a single isolated e or μ.
(ii) $p_T(e_1) > 14$ GeV, $p_T(e_2) > 14$ GeV or $p_T(e_1) > 25$ GeV, $p_T(e_2) > 10$ GeV for double e.
(iii) $p_T(\mu_1) > 14$ GeV, $p_T(\mu_2) > 14$ GeV or $p_T(\mu_1) > 18$ GeV, $p_T(\mu_2) > 10$ GeV for double μ.
(iv) $p_T(e_1/\mu_1) > 14$ GeV, $p_T(e_1/\mu_1) > 10$ GeV or $p_T(e_1/\mu_1) > 18$ GeV, $p_T(e_2/\mu_2) > 10$ GeV for $e + \mu$ events.

After these selections, events are classified in three signal regions, which are called SR0, SR1, SR2, following [65]. These have, respectively, at least 4 e/μ, exactly 3 e/μ and at least 1 τ_h, and exactly 2 e/μ and at least 2 τ_h. Events are then further classified into two categories, called no-Z and on-Z, which respectively veto against the presence of a Z boson or require the presence of Z boson. This is done by looking for an OSSF pair of leptons (e or μ) that yield invariant mass values in the $M_Z \pm 10$ GeV interval. The no-Z class is further divided into two regions, a and b,

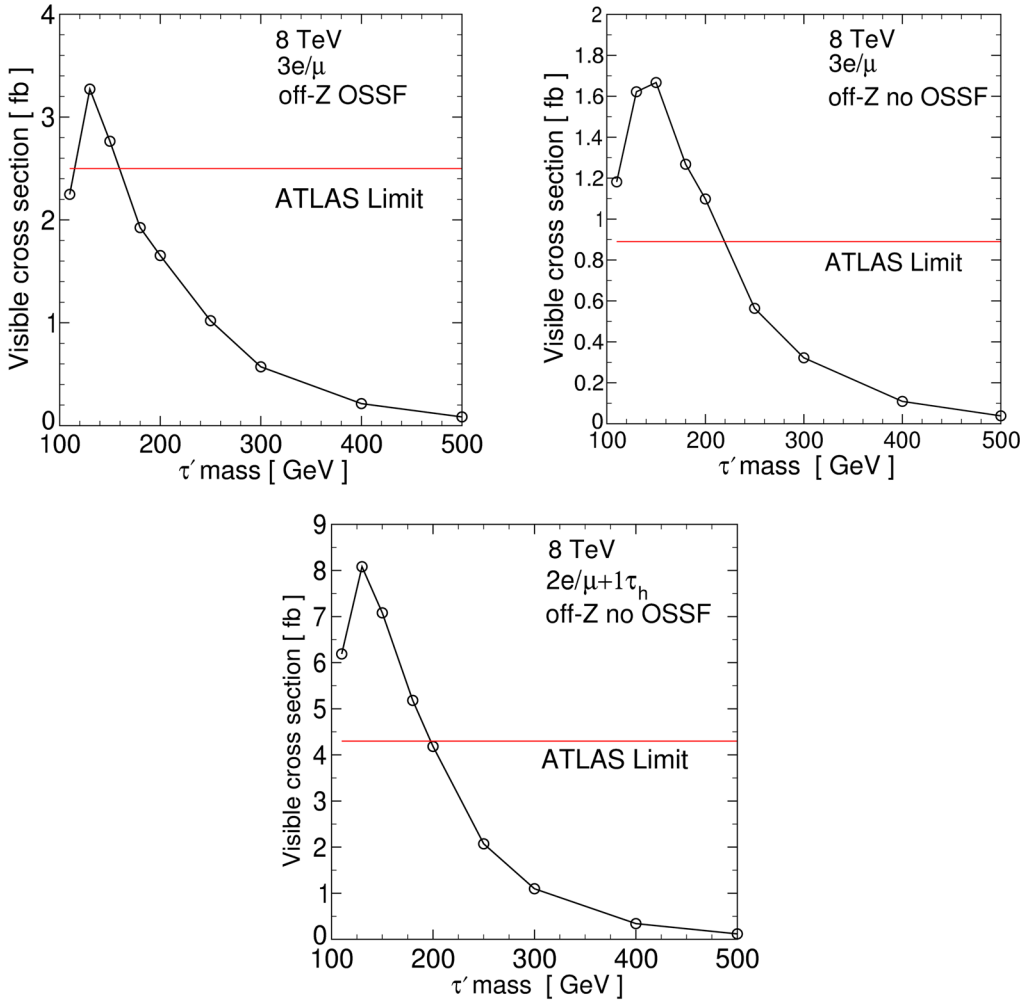

FIG. 4 (color online). Total visible cross sections σ_v, for the doublet VLL model, that pass selections: $\geq 3e/\mu$ off-Z OSSF (top left), $\geq 3e/\mu$ off-Z no-OSSF (top right), and $2e/\mu+\geq 1\tau_h$ off-Z no-OSSF (bottom left). The results are given as functions of $M_{\tau'} = M_{\nu'}$, at $\sqrt{s} = 8$ TeV, and are as given in Tables I and II. For comparison, the ATLAS limits at $\sqrt{s} = 8$ TeV and $\int L\,dt = 20.3$ fb^{-1} from Ref. [64] are represented by the horizontal red lines.

TABLE III. Total visible cross sections σ_v in the $\geq 4e/\mu$ channels that pass three different selection requirements for the signal regions, for the doublet VLL model, with $\sqrt{s} = 8$ TeV. The last line shows the ATLAS limit obtained at $\sqrt{s} = 8$ TeV with $\int L\,dt = 20.3$ fb^{-1} from [65].

$M_{\tau'}$ (GeV)	SR0noZa σ_v (fb)	SR0noZb σ_v (fb)	SR0Z σ_v (fb)
110	0.195	0.133	0.589
130	0.112	0.047	0.488
150	0.262	0.144	0.502
180	0.184	0.100	0.429
200	0.132	0.080	0.399
250	0.097	0.073	0.221
300	0.047	0.036	0.131
400	0.019	0.017	0.046
500	0.006	0.006	0.016
ATLAS limit	0.29	0.18	0.40

TABLE IV. Total visible cross sections σ_v in the $3e/\mu+\geq 1\tau_h$ channels that pass three different selection requirements for the signal regions, for the doublet VLL model, at $\sqrt{s} = 8$ TeV. The last line shows the ATLAS limit obtained at $\sqrt{s} = 8$ TeV with $\int L\,dt = 20.3$ fb^{-1} from [65].

$M_{\tau'}$ (GeV)	SR1noZa σ_v (fb)	SR1noZb σ_v (fb)	SR1Z σ_v (fb)
110	0.312	0.070	0.191
130	0.421	0.104	0.208
150	0.421	0.113	0.159
180	0.346	0.137	0.217
200	0.270	0.156	0.178
250	0.178	0.131	0.127
300	0.098	0.089	0.078
400	0.032	0.032	0.029
500	0.012	0.012	0.011
ATLAS limit	0.28	0.17	0.26

TABLE V. Total visible cross sections σ_v in the $2e/\mu+ \geq 2\tau_h$ channel that pass three different selection requirements for the signal regions, in the doublet VLL model, at $\sqrt{s} = 8$ TeV. The last line shows the ATLAS limit obtained at $\sqrt{s} = 8$ TeV with $\int L\,dt = 20.3$ fb^{-1} from [65].

$M_{\tau'}$ (GeV)	SR2noZa σ_v (fb)	SR2noZb σ_v (fb)	SR2Z σ_v (fb)
110	0.078	0.054	0.061
130	0.109	0.042	0.106
150	0.111	0.065	0.080
180	0.111	0.059	0.046
200	0.109	0.065	0.072
250	0.083	0.056	0.034
300	0.051	0.043	0.021
400	0.017	0.017	0.008
500	0.006	0.006	0.002
ATLAS limit	0.45	0.43	0.17

classified by $E_T^{\rm miss}$ and $m_{\rm eff}$ as defined in Table V of [65]. Hence the signal is studied in nine signal regions in all. Tables III, IV, and V show results from our simulation for the visible signal cross sections for the doublet VLL model in each category, as well as the corresponding ATLAS limits from Ref. [65].

It can be concluded from Tables III, IV, and V that the two signal regions with the best reach for the doublet VLL model are SR0Z (with at least 4 e/μ and a Z candidate) and SR1noZa (with exactly 3 e/μ, at least one τ_h, and no Z candidate). These results are shown in Fig. 5 as a function of $M_{\tau'} = M_{\nu'}$. As in the 3-lepton signal, we find that the predicted doublet VLL model visible cross section after cuts can exceed the ATLAS limit for masses below about 200 GeV. The same caveats apply as in the previous subsection, so we cannot claim an exclusion, but we simply note that these results are suggestive that such an exclusion may be possible with existing LHC data at $\sqrt{s} = 8$ TeV using these signal regions.

V. MORE INCLUSIVE FOUR-LEPTON SEARCHES AT $\sqrt{s} = 8$ TeV

The ATLAS searches of Ref. [65] were aimed at supersymmetric models, and therefore included cuts on $m_{\rm eff}$ and $E_T^{\rm miss}$. These cuts are not necessarily particularly appropriate for vectorlike lepton searches. Therefore, in this section we look at a different, simpler and more inclusive, strategy for 4-lepton searches to see if a better reach for the doublet VLL model can be achieved.

In the following, lepton candidates must satisfy

$$p_T(e,\mu,\tau_h) > 15\ \text{GeV}, \tag{5.1}$$

$$|\eta(e,\mu,\tau_h)| < 2.5, \tag{5.2}$$

$$\Delta R_{\ell,\ell'} > 0.1 \quad (\text{for each} \ell,\ell' = e,\mu,\tau_h). \tag{5.3}$$

$$\Delta R_{\ell j} > 0.3 \quad (\text{for each jet and} \ell = e,\mu,\tau_h). \tag{5.4}$$

We then require events to have at least 4 leptons, at least 2 of which must be e/μ, to satisfy a trigger requirement on the leading e/μ, and impose a veto of b-jets:

$$N(e,\mu,\tau_h) \geq 4, \tag{5.5}$$

$$N(e,\mu) \geq 2, \tag{5.6}$$

$$p_T(e_1/\mu_1) > 26\ \text{GeV}, \tag{5.7}$$

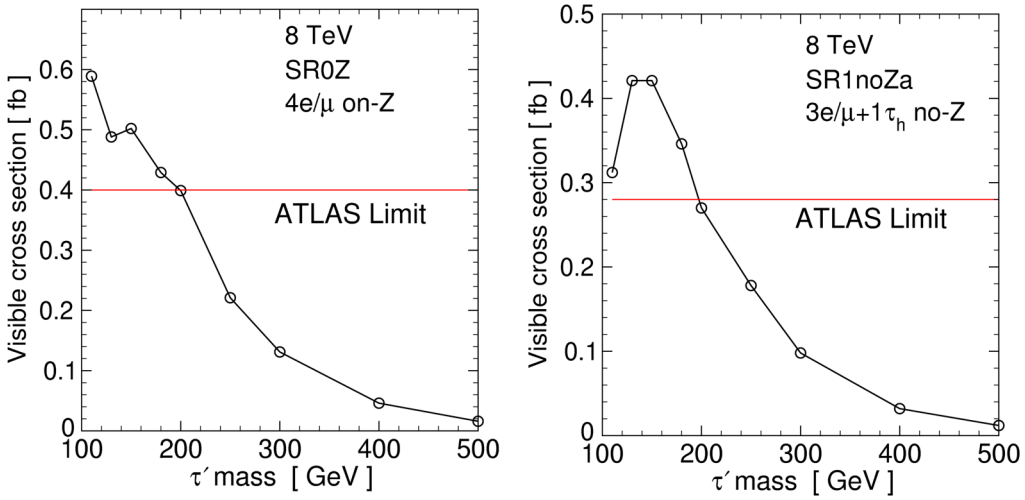

FIG. 5 (color online). Total visible cross sections σ_v, for the doublet VLL model, that pass selections $\geq 4e/\mu$ on-Z or SR0Z (left), and $3e/\mu+ \geq 1\tau_h$ no-Z or SR1noZa (right). The results are shown as a function of $M_{\tau'} = M_{\nu'}$, at $\sqrt{s} = 8$ TeV, and correspond to entries in Tables III and IV. Also, the ATLAS limits at $\sqrt{s} = 8$ TeV and $\int L\,dt = 20.3$ fb^{-1} from Ref. [65] are represented by the horizontal red lines.

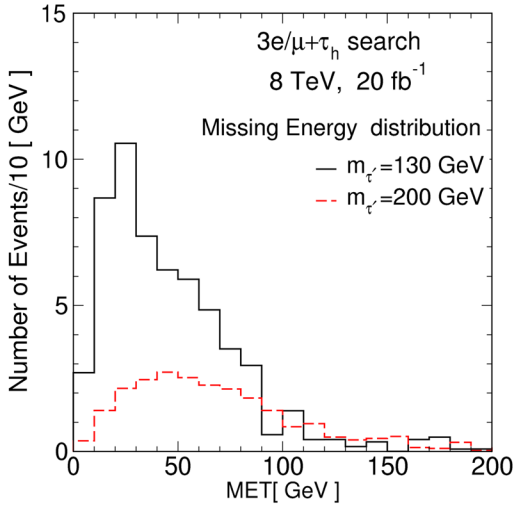

FIG. 6 (color online). The expected $E_T^{\rm miss}$ distribution at $\sqrt{s} = 8$ TeV in the $\geq 3e/\mu + 1\tau_h$ channel after inclusive event selection for the doublet VLL model with $M_{\tau'} = 130$ and 200 GeV. The distributions are normalized according to 20 fb^{-1} of integrated luminosity.

$$N_{b-\rm tag} = 0. \tag{5.8}$$

The last requirement is to help suppress $t\bar{t} + X$ backgrounds. We then consider 3 channels. The first one is $\geq 3e/\mu + 1\tau_h$, which requires at least three e/μ and at least one τ_h. Similarly we define a channel $\geq 2e/\mu + 2\tau_h$ with at least 2 e/μ and at least 2 τ_h, and a channel $\geq 4e/\mu$ by requiring at least 4 e/μ. (For simplicity, we avoid using $\geq$ sign in front of the number of τ_h requirement here.) Events that pass each of the selections just mentioned form categories that we call inclusive. Events which pass a further cut that there is no pair of OSSF leptons (e, μ) with $M_Z \pm 20$ are called no-Z. We do not include a separate on-Z category, because we found that the reach is typically very similar to the inclusive category. We also do not impose a cut on $E_T^{\rm miss}$, unlike the ATLAS 4-lepton signal region cuts, which were aimed at supersymmetry. The reason for this is illustrated in Fig. 6, which shows the $E_T^{\rm miss}$ distributions for the inclusive $\geq 3e/\mu + 1\tau_h$ channel, for two different mass values $M_{\tau'} = 130$ and 200 GeV. This distribution shows that $E_T^{\rm miss} < 100$ for most of the signal events if vectorlike leptons are pair produced according to the doublet VLL model and events are selected for four lepton channels.

The breakdown of background contributions and the total background cross section after the cuts for the 6 signal regions above, obtained using simulations as described in Sec. III with $\sqrt{s} = 8$ TeV, are given in Table VI. The largest backgrounds, even in the no-Z channels, come from ZZ, with subdominant contributions from hZ and WWZ, and WZ in the cases that use τ_h. The backgrounds from $t\bar{t}W$ and $t\bar{t}Z$, and $t\bar{t}h$ are significantly reduced by our use of a b-tag veto. The doublet VLL model signal cross sections for these 4-lepton search channels are given in Table VII for several different values of $M_{\tau'}$, along with the total background results from the previous table.

Using these results, we then calculate the median expected exclusion significance $Z_{\rm exc}$ for 20 fb^{-1} at $\sqrt{s} = 8$ TeV, assuming 10%, 20%, and 50% fractional uncertainty in the number of background events using Eq. (1.6). Hence $\Delta_b = 0.1b$, $0.2b$, and $0.5b$, where b is the mean total number of background events to pass any selection, and s is the corresponding number of signal events. We preferred to use this equation because in the real world it is impossible to know the backgrounds without uncertainty. This equation also allows us to calculate the significance even when b and s are small. Figure 7 shows the median expected exclusion significance predicted by Eq. (1.6) for the 6 different 4-lepton channels.

By looking at Fig. 7 we can say that the $\geq 3e/\mu + 1\tau_h$ channels predict the highest exclusion significance ($Z_{\rm exc}$) among the 4-lepton channels. We found $Z_{\rm exc} \geq 1.645$

TABLE VI. Background cross sections σ_b for four-lepton channels at $\sqrt{s} = 8$ TeV, after inclusive and no-Z selections as described in Sec. V.

	σ_b (fb) in $\geq 3e/\mu + 1\tau_h$		σ_b (fb) in $\geq 2e/\mu + 2\tau_h$		σ_b (fb) in $\geq 4e/\mu$	
SM backgrounds	inclusive	no-Z	inclusive	no-Z	inclusive	no-Z
$pp \to WZ$	0.0398	0.0000	0.0066	0.0066	0.0000	0.0000
$pp \to ZZ$	0.3753	0.0117	0.1909	0.0073	6.4511	0.0073
$pp \to t\bar{t}W$	0.0046	0.0034	0.0018	0.0017	0.0000	0.0000
$pp \to t\bar{t}Z$	0.0087	0.0016	0.0018	0.0010	0.0196	0.0005
$pp \to t\bar{t}h$	0.0038	0.0024	0.0027	0.0024	0.0019	0.0009
$pp \to hh$	0.0000	0.0000	0.0000	0.0000	0.0000	0.0000
$pp \to hZ$	0.0465	0.0017	0.0179	0.0017	0.0640	0.0012
$pp \to WWZ$	0.0094	0.0015	0.0015	0.0010	0.0503	0.0013
$pp \to WZZ$	0.0023	0.0002	0.0005	0.0001	0.0119	0.0002
$pp \to ZZZ$	0.0005	0.0000	0.0001	0.0000	0.0028	0.0000
Total background	0.4909	0.0225	0.2237	0.0218	6.6015	0.0115

TABLE VII. Signal and total background cross sections in the $\geq 3e/\mu + 1\tau_h$, $\geq 2e/\mu + 2\tau_h$ and $\geq 4e/\mu$ channels after selection through inclusive and no-Z requirements, for the doublet VLL model, at $\sqrt{s} = 8$ TeV.

	σ_s (fb) in $\geq 3e/\mu + 1\tau_h$		σ_s (fb) in $\geq 2e/\mu + 2\tau_h$		σ_s (fb) in $\geq 4e/\mu$	
$M_{\tau'}$ (GeV)	inclusive	no-Z	inclusive	no-Z	inclusive	no-Z
110	2.539	0.319	0.876	0.280	1.548	0.087
130	2.869	0.508	1.396	0.429	1.941	0.126
150	2.325	0.360	1.087	0.347	1.737	0.113
180	1.634	0.322	0.649	0.259	1.144	0.121
200	1.179	0.244	0.551	0.237	0.879	0.094
250	0.528	0.147	0.252	0.134	0.402	0.060
300	0.260	0.082	0.119	0.067	0.188	0.030
400	0.075	0.027	0.033	0.019	0.064	0.014
500	0.025	0.010	0.010	0.007	0.021	0.005
Total background	0.491	0.023	0.224	0.0218	6.602	0.012

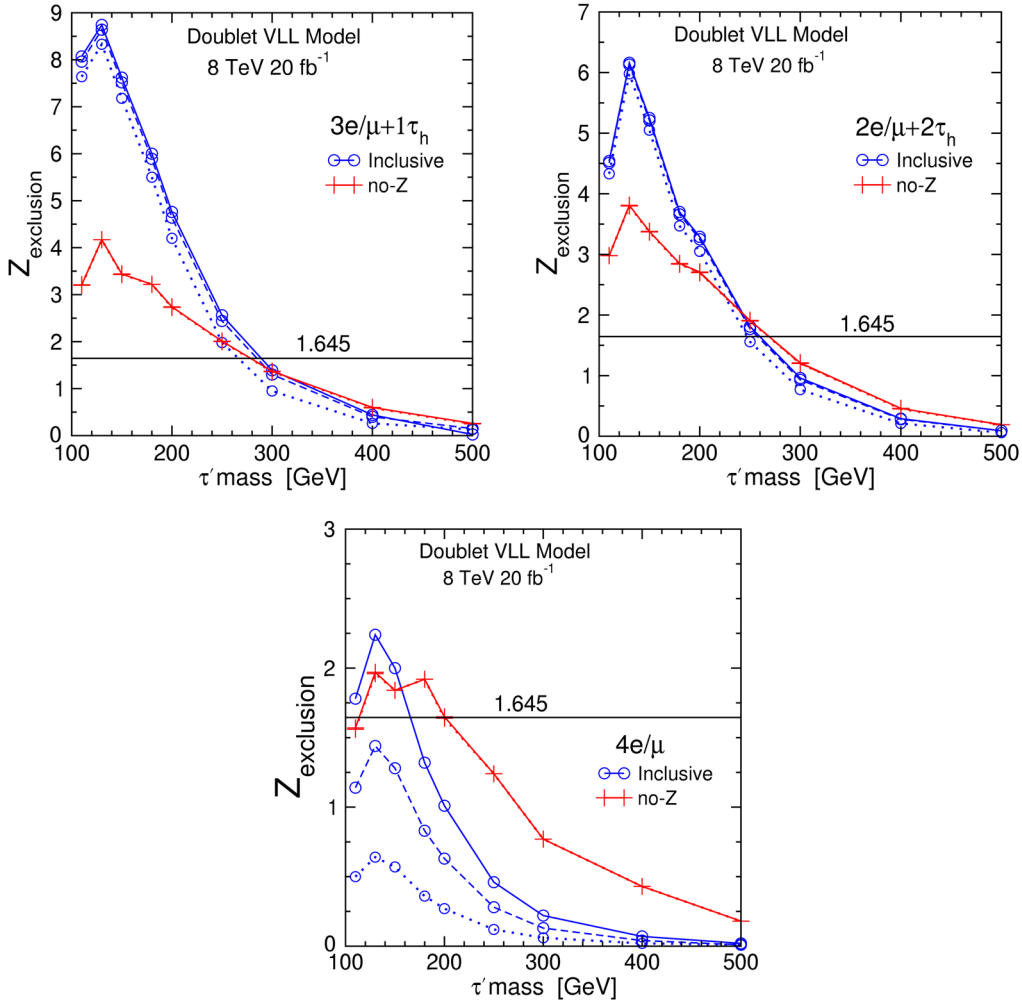

FIG. 7 (color online). Median expected significances for exclusion at $\int L\,dt = 20$ fb^{-1} in $\geq 3e/\mu + 1\tau_h$ (top left), $\geq 2e/\mu + 2\tau_h$ (top right), and $\geq 4e/\mu$ (bottom left) channels, for the doublet VLL model, as a function of $M_{\tau'} = M_{\nu'}$, at $\sqrt{s} = 8$ TeV, based on the results of Table VII. The different lines in each plot correspond to difference background variances, $\Delta_b = 0.1b$ (solid), $\Delta_b = 0.2b$ (dashed) and $\Delta_b = 0.5b$ (dotted), with blue lines (circle marks) for inclusive and red (plus marks) for no-Z on each figure. The horizontal black lines are $Z_{\text{exc}} = 1.645$ for 95% C.L.

corresponding to an expected 95% C.L. exclusion in the inclusive signal region when $M_{\tau'} \leq 265$ GeV, even with a fractional uncertainty in the background of up to 50%. When the background uncertainty is lower, the exclusion reach goes up to about 285 GeV. The no-Z channel has both smaller signals and smaller backgrounds, and also has exclusion power up to about $M_{\tau'} = 275$ GeV. For lower $M_{\tau'}$, the expected exclusion significance is much higher in the inclusive case than in the no-Z channel. Comparable, but slightly weaker, results are also found to hold for the $\geq 2e/\mu + 2\tau_h$ inclusive and no-Z channels. The $4e/\mu$ channels are seen to be considerably weaker. In particular, the inclusive region suffers from a very high background and the majority of that is from ZZ, while the no-Z $4e/\mu$ channel has a low signal cross section. As we expected from the nature of Eq. (1.6), lower exclusion significance decreases with increasing uncertainty in background events for a particular value of $M_{\tau'}$, in the case of the inclusive channels. For the low-background no-Z channels, the dependence on background uncertainty is very mild. We have not attempted a combination of the different signals, but this would clearly increase the exclusion power.

In this analysis, our expected exclusions are higher than what we got in the previous section where we considered analysis of the ATLAS 4-lepton signal regions for the VLL doublet model. There are several reasons for that. ATLAS considered $= 3e/\mu$ and $= 2e/\mu$ but we considered $\geq 3e/\mu$ and $\geq 2e/\mu$ events and that gave us more events in $\geq 3e/\mu + 1\tau_h$ and $\geq 2e/\mu + 2\tau_h$ channels. Our larger Z-mass window and b-jet veto tends to exclude more backgrounds. More importantly, the ATLAS 4-lepton signal regions used cuts on m_{eff} and on E_T^{miss}, which we did not find very useful, as illustrated above in Fig. 6. Since we do not have access to the data and our signal regions are quite different than those used by ATLAS and CMS multilepton searches, it is obvious that our results in this section should be considered only as indications of what might be excludable using existing $\sqrt{s} = 8$ TeV data, rather than as actual exclusions.

VI. MULTILEPTON SEARCHES AT $\sqrt{s} = 13$ TeV

We saw in the previous section that with the existing LHC data at $\sqrt{s} = 8$ TeV, it should be possible to set limits on the production of vectorlike leptons. In this section we perform a study of future prospects at $\sqrt{s} = 13$ TeV, estimating the integrated luminosity required to make a 95% C.L. exclusion, or an expected $Z_{\text{disc}} \geq 5$ discovery, as a function of $M_{\tau'}$ in both the doublet and singlet VLL models. To do that, we define 4-lepton and 5-lepton signal regions, use simulations to find the visible cross sections after cuts, and then solve $Z_{\text{exc}} = 1.645$ using Eq. (1.6) or $Z_{\text{disc}} = 5$ using Eq. (1.4) for the integrated luminosity. Our 4-lepton signal regions are the same as in the previous section, and are referred to as $\geq 3e/\mu + 1\tau_h$, $\geq 2e/\mu + 2\tau_h$ and $\geq 4e/\mu$. We also consider 5-lepton signal regions, which essentially require one extra e/μ, and will be called $\geq 4e/\mu + 1\tau_h$, $\geq 3e/\mu + 2\tau_h$ and $\geq 5e/\mu$. In each case, we consider inclusive and no-Z channels. For our study, we generated 100,000 signal events with $\sqrt{s} = 13$ TeV, for each of $M_{\tau'} = 110$, 130, 150, 180, 200, 250, 300, 400, and 500 GeV. We have also generated the backgrounds at $\sqrt{s} = 13$ TeV and studied their contributions in each of these channels. We consider the doublet VLL model first, and then study the prospects for the singlet VLL model as well as a more optimistic variant of it.

A. Four-lepton searches for the doublet VLL model

At $\sqrt{s} = 13$ TeV, we selected events using the same requirements as described in the previous section. The individual background cross sections after cuts are listed in Table VIII for each of the 6 signal regions. The doublet VLL model signal cross sections are given in Table IX for various masses $M_{\tau'}$. By solving Eqs. (1.6) and (1.4) we get

TABLE VIII. Background cross sections σ_b for 4-lepton channels at $\sqrt{s} = 13$ TeV, after inclusive and no-Z selections as described in Sec. V.

	σ_b (fb) in $\geq 3e/\mu + 1\tau_h$		σ_b (fb) in $\geq 2e/\mu + 2\tau_h$		σ_b (fb) in $\geq 4e/\mu$	
SM backgrounds	inclusive	no-Z	inclusive	no-Z	inclusive	no-Z
$pp \to WZ$	0.0637	0.0000	0.0127	0.0127	0.0000	0.0000
$pp \to ZZ$	0.7840	0.0242	0.4555	0.0302	14.7263	0.0121
$pp \to t\bar{t}W$	0.0080	0.0057	0.0028	0.0025	0.0000	0.0000
$pp \to t\bar{t}Z$	0.0249	0.0045	0.0059	0.0033	0.0508	0.0014
$pp \to t\bar{t}h$	0.0071	0.0049	0.0071	0.0056	0.0052	0.0026
$pp \to hh$	0.0012	0.0004	0.0008	0.0004	0.0016	0.0004
$pp \to hZ$	0.1377	0.0084	0.0588	0.0051	0.2418	0.0067
$pp \to WWZ$	0.0193	0.0034	0.0025	0.0017	0.0986	0.0026
$pp \to WZZ$	0.0062	0.0004	0.0015	0.0004	0.0423	0.0005
$pp \to ZZZ$	0.0030	0.0001	0.0013	0.0002	0.0282	0.0002
Total background	1.055	0.0520	0.549	0.0619	15.1950	0.0265

TABLE IX. Signal and total background cross sections in the $\geq 3e/\mu + 1\tau_h$, $\geq 2e/\mu + 2\tau_h$ and $\geq 4e/\mu$ channels after selection through inclusive and no-Z requirements, for the doublet VLL model, at $\sqrt{s} = 13$ TeV.

	σ_s (fb) in $\geq 3e/\mu + 1\tau_h$		σ_s (fb) in $\geq 2e/\mu + 2\tau_h$		σ_s (fb) in $\geq 4e/\mu$	
$M_{\tau'}$ (GeV)	inclusive	no-Z	inclusive	no-Z	inclusive	no-Z
110	3.048	0.490	1.353	0.636	2.632	0.000
130	5.126	0.782	2.402	0.729	2.877	0.302
150	4.123	0.533	1.896	1.008	3.050	0.214
180	2.712	0.538	1.158	0.670	1.913	0.193
200	2.173	0.533	0.958	0.507	1.558	0.177
250	1.037	0.267	0.495	0.312	0.740	0.108
300	0.549	0.178	0.257	0.178	0.456	0.098
400	0.188	0.068	0.095	0.085	0.170	0.036
500	0.081	0.033	0.035	0.033	0.066	0.016
Total background	1.055	0.052	0.549	0.062	15.195	0.027

the median expected integrated luminosities needed for 95% C.L. exclusion and $Z_{\rm disc} > 5$ discovery, as a function of $M_{\tau'}$. These results are shown in Fig. 8, for the cases of assumed 10%, 20%, and 50% fractional uncertainties in the background. Just as in the $\sqrt{s} = 8$ TeV case, we find that the reach is best in the channels that include at least one τ_h candidates.

Assuming the signal is absent, then with 10 fb^{-1} one expects to be able to make a 95% C.L. exclusion for $M_{\tau'}$ up to about 270 GeV, using the no-Z version of either of the $\geq 3e/\mu + 1\tau_h$ or $\geq 2e/\mu + 2\tau_h$ channels. This is true even if the assumed fractional uncertainty in the background is as large as 50%, simply because the no-Z background levels are small. The inclusive $\geq 3e/\mu + 1\tau_h$ channel seems to do slightly better for exclusion with 10 fb^{-1}, but only if the fractional uncertainty in the background is less than 20%. With 100 fb^{-1}, the no-Z channels are clearly better, and can exclude up to about $M_{\tau'} = 440$ GeV (or 400 GeV), provided that the fractional uncertainty in the background is not more than 20% (or 50%).

Under the same circumstances, a discovery of the doublet VLL model could be possible up to about $M_{\tau'} = 300$ GeV with 100 fb^{-1}, using either the no-Z selection for either of the $\geq 3e/\mu + 1\tau_h$ or $\geq 2e/\mu + 2\tau_h$ channels. The discovery reach in these channels degrades to about 210 GeV if $\Delta_b = 0.5b$. In general, the inclusive search is seen to be better at low masses where the signal cross section is large enough to overcome the significant backgrounds, while the no-Z channel performs much better at high masses.

Also, because of the higher background, the inclusive channels tend to be more sensitive to a given assumed level of fractional background uncertainties than the no-Z channels. With an assumption of a 50% fractional uncertainty in the background, the exclusion reach is completely eliminated for $M_{\tau'}$ above 400 GeV. The discovery reach similarly is absent for $M_{\tau'}$ above 300 GeV if the fractional uncertainty in the background is larger than 20%. The real-world background uncertainties will likely be larger for the $2\tau_h$ cases than the $1\tau_h$ cases. It may well also be possible to combine these channels to enhance the significance of an exclusion or discovery, but we do not attempt this here. The $\geq 4e/\mu$ search with a no-Z requirement is seen to be much less powerful, and the inclusive channel (not shown) is quite weak as it suffers from a comparatively very large ZZ background. Similarly to the $\sqrt{s} = 8$ TeV inclusive search of the previous section, we found that an on-Z selection (also not shown) would not do any better than the inclusive selection.

B. Five-lepton searches for the doublet VLL model

In this section, we consider 5-lepton search channels for the doublet VLL model. These have the advantage that the backgrounds tend to be extremely small. We use the same criteria for lepton identification and isolation as in Sec. V, and again require as a trigger at least one high-p_T electron or muon, as in Eq. (5.7). We then define three channels $\geq 4e/\mu + 1\tau_h$, $\geq 3e/\mu + 2\tau_h$ and $\geq 5e/\mu$. For each of these, we further consider the inclusive and no-Z categories, as before.

The individual backgrounds are given in Table X. We note that all of the backgrounds are quite small, amounting to only a few events expected even in 1000 fb^{-1} in the inclusive cases, and fewer than 1 event in 1000 fb^{-1} in the no-Z 5-lepton cases. In some background channels, our simulations did not find any events that passed all of the selection criteria. The $pp \to ZZ$ and $pp \to t\bar{t}Z$ backgrounds are the largest in the inclusive cases for $\geq 4e/\mu + 1\tau_h$ and $\geq 3e/\mu + 2\tau_h$, but these are effectively eliminated if the no-Z requirement is included. We note that these backgrounds rely on the rate for jets to fake τ_h, which we took to be 0.001 as noted above. In the real world, these backgrounds will have to be determined for the relevant topologies by using control regions.

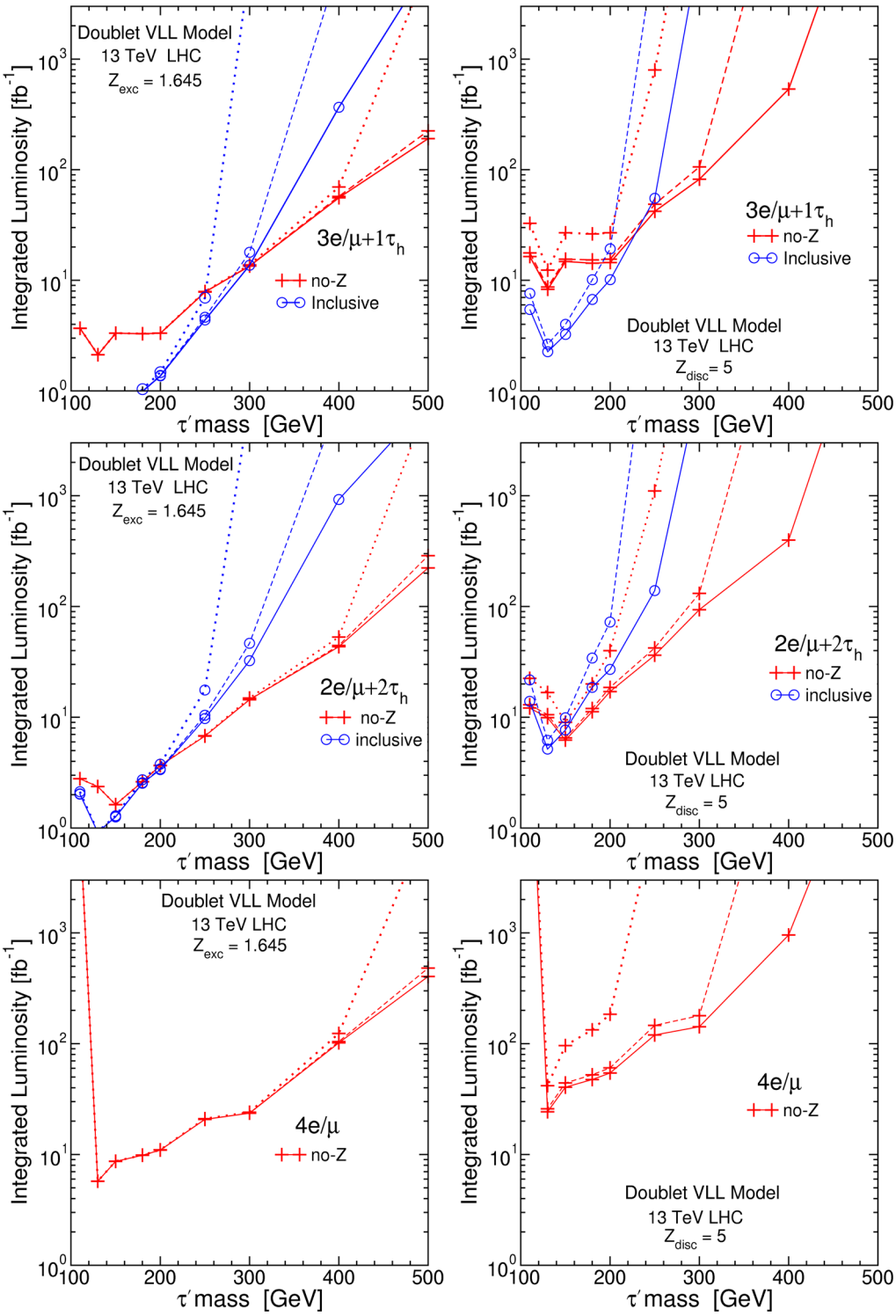

FIG. 8 (color online). Integrated luminosity needed for a median expected significance $Z_{\rm exc} \geq 1.645$ for exclusion (left) and $Z_{\rm disc} \geq 5$ for discovery (right) in $\geq 3e/\mu + 1\tau_h$, $\geq 2e/\mu + 2\tau_h$, and $\geq 4e/\mu$ channels, for the doublet VLL model, as a function of $M_{\tau'} = M_{\nu'}$, at $\sqrt{s} = 13$ TeV, based on the results of Table IX. The different lines correspond to assumed background uncertainties $\Delta_b = 0.1$b (solid), $\Delta_b = 0.2$b (dashed) and $\Delta_b = 0.5$b (dotted), with blue lines (circle marks) for inclusive and red (plus marks) for no-Z on each figure.

For the signal, the contributions come mostly from $h\tau Z\tau$, $Z\tau Z\tau$ and $W\tau Z\tau$ events resulting from vectorlike lepton production. Results are shown in Table XI as a function of $M_{\tau'}$ for the doublet VLL model. In these simulations, we forced the Z and W to decay leptonically (including to τ leptons) for better statistics. Inclusive and on-Z requirements give essentially the same results, so we do not consider separately an on-Z search.

TABLE X. Background cross sections σ_b after inclusive and no-Z selections, for five lepton channels at $\sqrt{s} = 13$ TeV.

	σ_b (fb) in $\geq 4e/\mu + 1\tau_h$		σ_b (fb) in $\geq 5e/\mu$		σ_b (fb) in $\geq 3e/\mu + 2\tau_h$	
SM backgrounds	inclusive	no-Z	inclusive	no-Z	inclusive	no-Z
$pp \to ZZ$	0.00202	0	0	0	0.00202	0
$pp \to t\bar{t}W$	0	0	0	0	0.00026	0.00013
$pp \to t\bar{t}Z$	0.00215	0.00013	0	0	0.00124	0.00007
$pp \to t\bar{t}h$	0	0	0	0	0.00150	0.00075
$pp \to WWZ$	0.00012	0	0	0	0.00003	0
$pp \to WZZ$	0.00076	0.000004	0.00498	0.000015	0.00019	0.0000073
$pp \to ZZZ$	0.00044	0.000004	0.00150	0.000002	0.00008	0.0000031
Total background	0.00548	0.00014	0.00648	0.000017	0.00533	0.00096

Results for the luminosities needed to achieve a median expected $Z_{\rm exc} \geq 1.645$ (95% C.L. exclusion) or $Z_{\rm exc} \geq 5$ (discovery) are presented in Fig. 9. The 5-lepton search strategy is statistics limited, rather than background limited. Therefore, for 10 fb^{-1} of integrated luminosity, these channels are not competitive with the 4-lepton searches of the previous section. Clearly, very high integrated luminosities are required if a no-Z search is performed, because of the very low signal yields. The best search strategy for achieving a 95% C.L. exclusion seems to be the $\geq 4e/\mu + 1\tau_h$ inclusive search, which with 100 fb^{-1} can exclude up to $M_{\tau'} = 340$ GeV even if the fractional background uncertainty is taken to be 50%. However, for smaller background uncertainties this search is less effective than the 4-lepton no-Z searches described in the previous section (compare Fig. 7).

Similarly, the potential for doublet VLL discovery using the 5-lepton searches is somewhat worse than in the 4-lepton search of the previous section if one assumes that the background uncertainties in both cases are taken to be 10% or lower, but the situation is reversed if the assumed fractional background uncertainties are higher. With 100 fb^{-1}, the $\geq 4e/\mu + 1\tau_h$ inclusive search could discover the doublet VLL model for masses up to about $M_{\tau'} = 250$ GeV, even if the fractional uncertainty in the background is 50%. With an integrated luminosity of 1000 fb^{-1}, there is a possibility of discovering the doublet VLL model up to $M_{\tau'} = 400$ GeV in the same channel, provided that the background uncertainty is 10% or lower. The other 5-lepton channels provide somewhat less discovery reach.

C. Four-lepton searches for the singlet VLL model

In the singlet VLL model we only have the production of $\tau'^+\tau'^-$. Hence the signal cross section that contributes to the visible final states is much smaller than for the doublet VLL model. The challenge is illustrated by Fig. 10, in which the plot on the left shows the dependence on $M_{\tau'}$ of the total branching fraction of $\tau'^+\tau'^-$ into different individual multilepton channels $\geq 3e/\mu$, $\geq 4e/\mu$, $\geq 3e/\mu + 1\tau_h$ and $\geq 2e/\mu + 2\tau_h$, and the plot on right shows the cross section $\times$ BR, before putting in any cuts or detection efficiencies. From Fig. 10, it is evident that a 3-lepton search gives the biggest contribution in signal cross section, but that suffers from a large background. We therefore will concentrate on 4-lepton and 5-lepton searches.

In Fig. 11, we show results for the 4-lepton channels $\geq 3e/\mu + 1\tau_h$ and $\geq 2e/\mu + 2\tau_h$, again before any cuts or

TABLE XI. Signal and background cross sections for the doublet VLL model, at $\sqrt{s} = 13$ TeV in the $\geq 4e/\mu + 1\tau_h$, $\geq 3e/\mu + 2\tau_h$ and $\geq 5e/\mu$ channels after selection through inclusive and no-Z requirements.

	σ_s (fb) in $\geq 4e/\mu + 1\tau_h$		σ_s (fb) in $\geq 3e/\mu + 2\tau_h$		σ_s (fb) in $\geq 5e/\mu$	
$M_{\tau'}$ (GeV)	inclusive	no-Z	inclusive	no-Z	inclusive	no-Z
110	0.156	0.01104	0.091	0.01060	0.081	0.00029
130	0.382	0.01682	0.204	0.00950	0.204	0.00569
150	0.315	0.00799	0.176	0.01275	0.176	0.00345
180	0.217	0.00842	0.112	0.00882	0.138	0.00188
200	0.169	0.00507	0.081	0.00749	0.106	0.00146
250	0.088	0.00314	0.042	0.00446	0.057	0.00085
300	0.046	0.00257	0.021	0.00326	0.032	0.00058
400	0.015	0.00086	0.007	0.00120	0.011	0.00032
500	0.006	0.00037	0.002	0.00044	0.005	0.00016
Total background	0.00548	0.00014	0.00533	0.00096	0.00648	0.000017

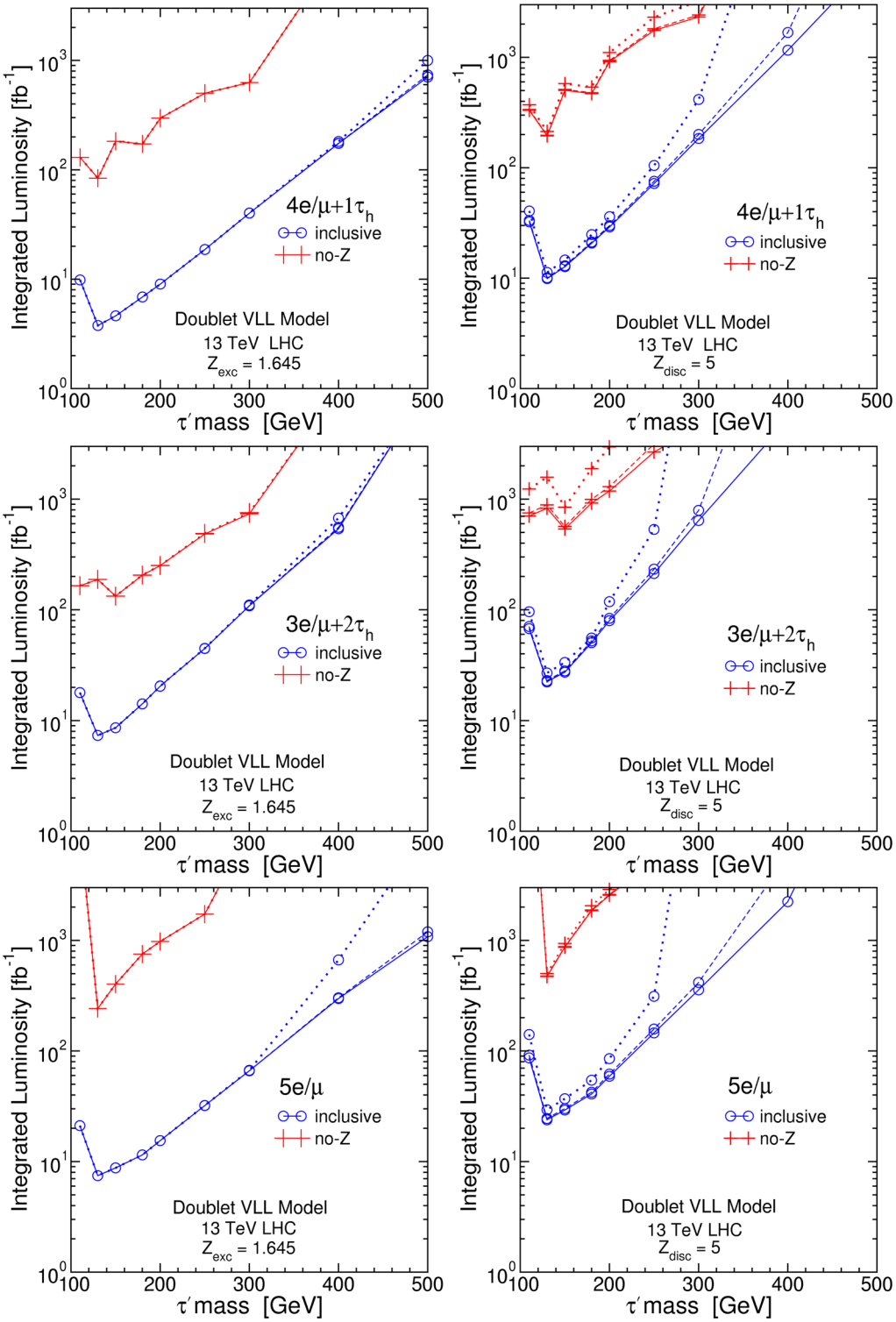

FIG. 9 (color online). Integrated luminosity needed for a median expected significance $Z_{\rm exc} \geq 1.645$ for 95% C.L. exclusion (left) and $Z_{\rm disc} \geq 5$ for discovery (right) in $\geq 4e/\mu + 1\tau_h$, $\geq 3e/\mu + 2\tau_h$, and $\geq 5e/\mu$ channels, for the doublet VLL model, as a function of $M_{\tau'} = M_{\nu'}$, at $\sqrt{s} = 13$ TeV, based on the results of Table XI. In the figures different lines correspond to $\Delta_b = 0.1$b (solid), $\Delta_b = 0.2$b (dashed) and $\Delta_b = 0.5$b (dotted), with blue lines (circle marks) for inclusive, red (plus marks) for no-Z on each figure.

detection efficiencies, and this time allowing the branching ratios of τ' into the three possible final states $Z\tau$ and $h\tau$ and $W\nu$ to float, subject to the constraint $\mathrm{BR}(\tau' \to Z\tau) + \mathrm{BR}(\tau' \to h\tau) + \mathrm{BR}(\tau' \to W\nu) = 1$. The effects of leptonic τ decays have been included. Within this plane of more general possibilities, the thick red curve shows the prediction of the singlet VLL model (following from the results shown in Fig. 3), and the other contour lines have

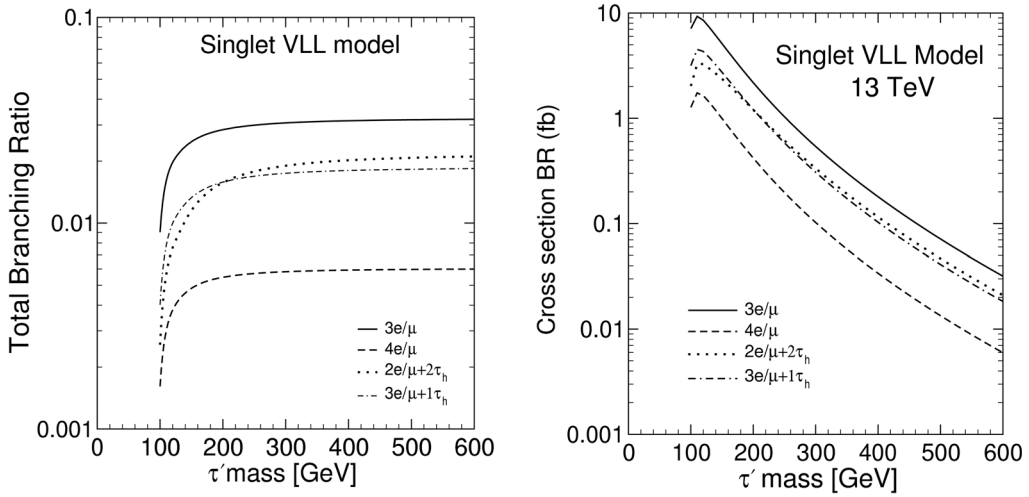

FIG. 10. The total branching ratio (left) and cross section × branching ratio (right) that contribute to different channels are shown as a function of τ' mass for singlet VLL model. In the plot at right, the cross sections predicted by the singlet VLL model at $\sqrt{s} = 13$ TeV are used.

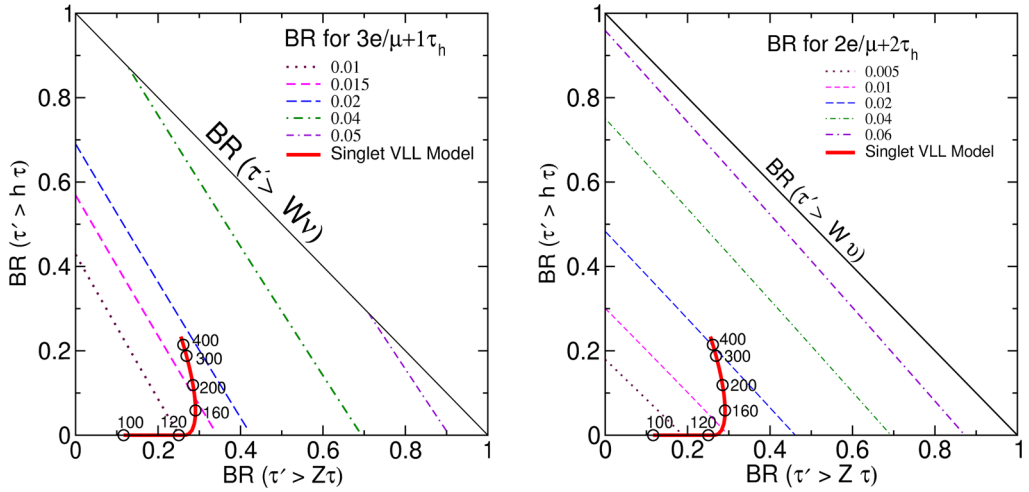

FIG. 11 (color online). Contour lines for total branching ratio of $\tau'^{+}\tau'^{-}$ into $\geq 3e/\mu + 1\tau_h$ (left) and $\geq 2e/\mu + 2\tau_h$ (right) channels are shown in the plane of BR($\tau' \to h\tau$) and BR($\tau' \to Z\tau$), assuming BR($\tau' \to W\nu$) = 1-BR($\tau' \to h\tau$)-BR($\tau' \to Z\tau$). The prediction of the singlet VLL model is shown by the thick red curve, with circles corresponding to $M_{\tau'} = 100$, 120, 160, 200, 300, 400 GeV.

TABLE XII. Signal and background cross sections in the $\geq 3e/\mu + 1\tau_h$, $\geq 2e/\mu + 2\tau_h$ and $\geq 4e/\mu$ channels after selecting events through inclusive and no-Z requirements, for the singlet VLL model, at $\sqrt{s} = 13$ TeV.

	σ_s (fb) in $\geq 3e/\mu + 1\tau_h$		σ_s (fb) in $\geq 2e/\mu + 2\tau_h$		σ_s (fb) in $\geq 4e/\mu$	
$M_{\tau'}$ (GeV)	inclusive	no-Z	inclusive	no-Z	inclusive	no-Z
120	0.0672	0.0027	0.0143	0.0023	0.0528	0.0007
130	0.0811	0.0035	0.0208	0.0027	0.0644	0.0011
140	0.0809	0.0037	0.0225	0.0050	0.0679	0.0012
150	0.0819	0.0060	0.0215	0.0043	0.0651	0.0016
160	0.0758	0.0047	0.0210	0.0057	0.0565	0.0016
180	0.0627	0.0057	0.0208	0.0052	0.0491	0.0021
200	0.0469	0.0047	0.0161	0.0055	0.0404	0.0021
250	0.0259	0.0038	0.0094	0.0038	0.0230	0.0017
300	0.0150	0.0026	0.0056	0.0025	0.0141	0.0010
Total background	1.055	0.052	0.549	0.062	15.195	0.026

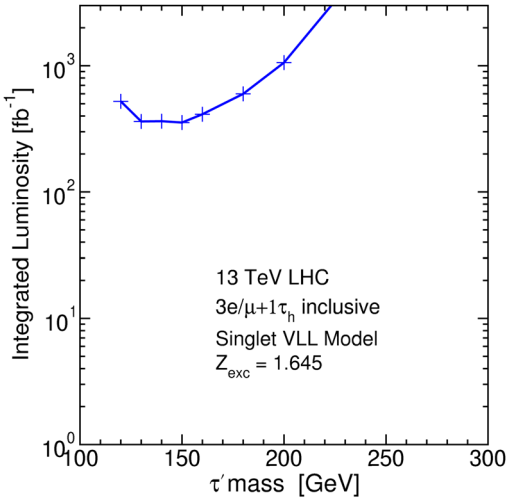

FIG. 12 (color online). Integrated luminosity needed for a median expected $Z_{\rm exc} \geq 1.645$ (95% C.L.) exclusion in the inclusive $\geq 3e/\mu + 1\tau_h$ channel, for the singlet VLL model, as a function of $M_{\tau'}$, at $\sqrt{s} = 13$ TeV, based on the results of Table XII. The line with plus symbols represents the required luminosity in the most optimistic case of no uncertainty in the background cross section ($\Delta_b = 0$). We do not find any prospects for exclusion if the fractional uncertainty in the background is 10% or higher.

constant branching ratios of $\tau'^+\tau'^-$ into $\geq 3e/\mu + 1\tau_h$ and $\geq 2e/\mu + 2\tau_h$. The predicted large $\mathrm{BR}(\tau' \to W\nu)$ in the single VLL model, especially for low $M_{\tau'}$ is seen to be the reason for low signal yields for 4-lepton and 5-lepton channels.

In the following, we performed 4-lepton searches by generating events using the same cuts and selections as we did for the doublet VLL model at $\sqrt{s} = 13$ TeV in Sec. VI A. The results for individual backgrounds were already listed above in Table VIII. The signal and total background cross sections to pass the inclusive and no-Z selections are listed in Table XII, for various $M_{\tau'}$. We find that the no-Z selection is not effective for the purposes of setting a 95% C.L. exclusion or claim a discovery in 4-lepton searches, for the singlet VLL model. Even in the case of the inclusive selections, we found that in the singlet VLL model no reasonable integrated luminosity would be able to set a 95% C.L. exclusion or claim a discovery in $\geq 4e/\mu$, $\geq 2e/\mu + 2\tau_h$ and $\geq 3e/\mu + 1\tau_h$ channels at 13 TeV, if the uncertainty in the background is 10%. This is because in this case the background cross section is always greater than the signal cross section by more than a factor of 10. However, in the most optimistic possible case that there is no uncertainty at all in the background cross section, then it would be possible to set a 95% C.L. exclusion in $\geq 3e/\mu + 1\tau_h$ channel with 350 fb^{-1} luminosity for $130\ \mathrm{GeV} < M_{\tau'} < 150\ \mathrm{GeV}$, as shown in Fig. 12. With 1000 fb^{-1}, the exclusion reach in this case would extend up to about $M_{\tau'} = 200$ GeV.

In view of the rather pessimistic nature of these results, we now study a more optimistic variant of the singlet VLL model in which $\mathrm{BR}(\tau' \to Z\tau) = 1$ is forced, but the production cross section is not changed. We emphasize that this is somewhat arbitrary, as we do not have in mind a specific model that actually makes this prediction, although this scenario is at least consistent in the sense that the couplings involved in the production are different from those involved in the decays. The signal cross sections to pass the inclusive and no-Z selections in this case are given in Table XIII. We find that in this case, it is possible to set 95% exclusions in the $\geq 3e/\mu + 1\tau_h$ and $\geq 2e/\mu + 2\tau_h$ channels with the inclusive search (and also with the no-Z search, although that will require a much higher luminosity). Figure 13 shows the integrated luminosity needed to set $Z_{\rm exc} \geq 1.645$ exclusion in in these two channels. We found that it is possible to obtain a 95% C.L. exclusion for $M_{\tau'} \leq 190$ GeV with 100 fb^{-1} in the $\geq 3e/\mu + 1\tau_h$ inclusive search with 10% uncertainty in the background events.

TABLE XIII. Signal and background cross sections in the $\geq 3e/\mu + 1\tau_h$, $\geq 2e/\mu + 2\tau_h$ and $\geq 4e/\mu$ channels after selecting events through inclusive and no-Z requirements, for the modified singlet VLL model with $\mathrm{BR}(\tau' \to Z\tau) = 1$ at $\sqrt{s} = 13$ TeV.

	σ_s (fb) in $\geq 3e/\mu + 1\tau_h$		σ_s (fb) in $\geq 2e/\mu + 2\tau_h$		σ_s (fb) in $\geq 4e/\mu$	
$M_{\tau'}$ (GeV)	inclusive	no-Z	inclusive	no-Z	inclusive	no-Z
120	0.2898	0.0043	0.1341	0.0043	0.3071	0.0000
130	0.3449	0.0133	0.1891	0.0100	0.3217	0.0000
140	0.3393	0.0130	0.1865	0.0285	0.3057	0.0000
150	0.4048	0.0288	0.1685	0.0164	0.2733	0.0021
160	0.3386	0.0099	0.1520	0.0215	0.2081	0.0017
180	0.3014	0.0188	0.1391	0.0144	0.1921	0.0022
200	0.2052	0.0084	0.1026	0.0130	0.1784	0.0038
250	0.1181	0.0059	0.0501	0.0079	0.1019	0.0024
300	0.0728	0.0044	0.0257	0.0047	0.0642	0.0009
Total background	1.055	0.052	0.549	0.062	15.195	0.026

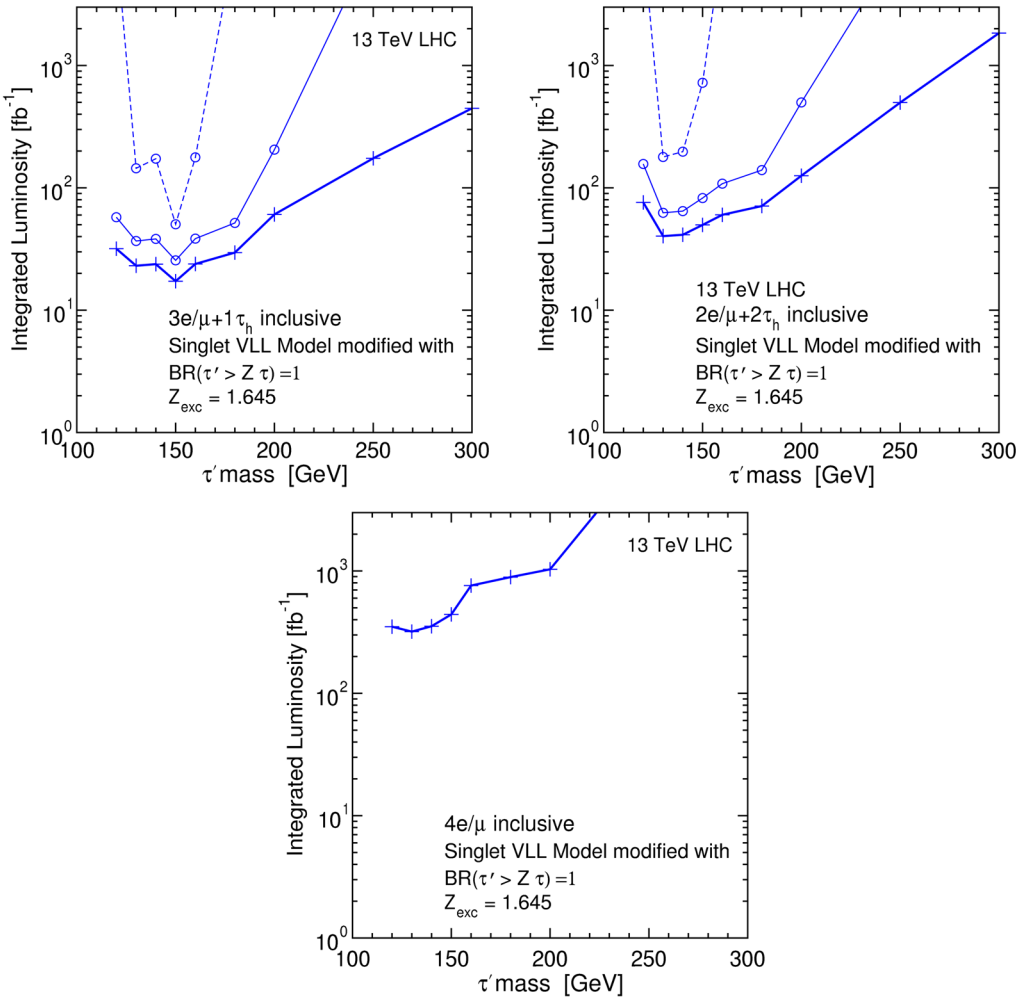

FIG. 13 (color online). Integrated luminosities needed for $Z_{\rm exc} = 1.645$ (95% C.L.) exclusion, in the inclusive $\geq 3e/\mu + 1\tau_h$ and $\geq 2e/\mu + 2\tau_h$ and $\geq 4e/\mu$ channels, for the modified singlet VLL model with $\mathrm{BR}(\tau' \to Z\tau) = 1$, as a function of $M_{\tau'}$, at $\sqrt{s} = 13$ TeV, based on the results from Table XIII. The different lines in each plot correspond to assumed background uncertainties $\Delta_b = 0$ (thicker solid, with + signs), $\Delta_b = 0.1b$ (solid, with circles) and $\Delta_b = 0.2b$ (dashed, with circles).

However, we found that it is not possible to satisfy the $Z_{\rm disc} \geq 5$ discovery criteria in the 4-lepton channels at $\sqrt{s} = 13$ TeV, for any reasonable integrated luminosity and any value of $M_{\tau'}$.

D. Five-lepton searches for the singlet VLL model

In this section, we consider the 5-lepton channels at $\sqrt{s} = 13$ TeV for the singlet VLL model to study the prospectives for exclusion or discovery, in the same manner as we did in Sec. VI B for the doublet VLL model. The individual backgrounds were already given above in Table X. The visible signal cross sections after cuts are quite small, even to pass the inclusive selections, as can be seen from Table XIV. Note that the three individual 5-lepton channels have comparable signal and background levels. Therefore, because of the low cross section yields,

TABLE XIV. Signal and total background cross sections in the $\geq 4e/\mu + 1\tau_h$, $\geq 3e/\mu + 2\tau_h$ and $\geq 5e/\mu$ channels after inclusive selections, for the singlet VLL model, at $\sqrt{s} = 13$ TeV.

$M_{\tau'}$ (GeV)	σ_s (fb) in $\geq 4e/\mu + 1\tau_h$	σ_s (fb) in $\geq 3e/\mu + 2\tau_h$	σ_s (fb) in $\geq 5e/\mu$
120	0.00285	0.00071	0.00186
130	0.00393	0.00113	0.00246
140	0.00420	0.00123	0.00293
150	0.00417	0.00134	0.00310
160	0.00399	0.00138	0.00302
180	0.00343	0.00142	0.00277
200	0.00294	0.00120	0.00211
250	0.00176	0.00082	0.00141
300	0.00094	0.00049	0.00080
Total background	0.0055	0.0065	0.0053

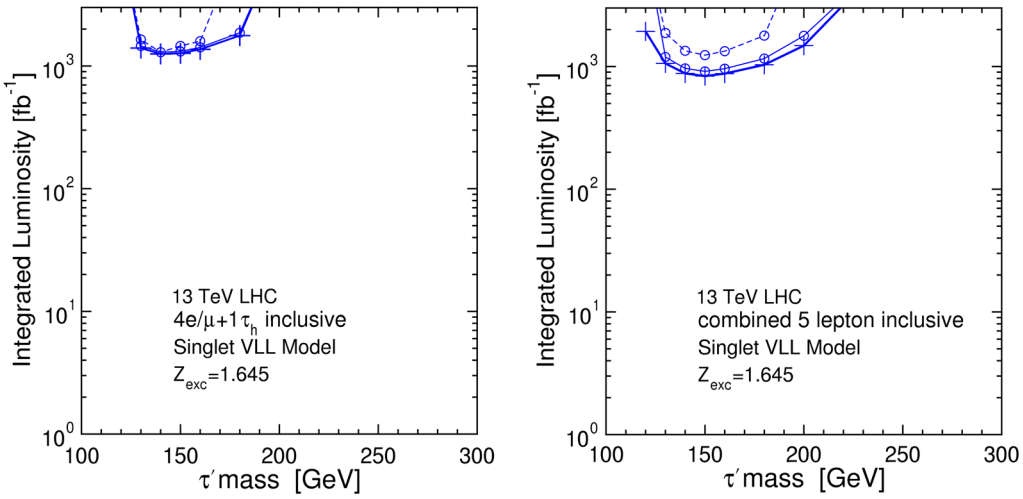

FIG. 14 (color online). Integrated luminosities needed for median expected $Z_{\rm exc} = 1.645$ (95% C.L.) exclusion in the $\geq 4e/\mu + 1\tau_h$ and combined 5-lepton inclusive searches, for the singlet VLL model, as a function of $M_{\tau'}$, at $\sqrt{s} = 13$ TeV, based on the results from Table XIV. The different lines in each plot correspond to assumed background uncertainties $\Delta_b = 0$ (thicker solid, with + signs), $\Delta_b = 0.1b$ (solid, with circles) and $\Delta_b = 0.2b$ (dashed, with circles).

we consider not only the individual $\geq 4e/\mu + 1\tau_h$, $\geq 3e/\mu + 2\tau_h$ and $\geq 5e/\mu$ inclusive cross sections, but also their combination given by the sum of the three channels. We then find that with a very high integrated luminosity, of 1000 fb^{-1}, it may be possible to set a 95% C.L. exclusion for a narrow range of 140 GeV $< M_{\tau'} <$ 165 GeV, using the $\geq 4e/\mu + 1\tau_h$ channel or the combined 5-lepton channel. These results are shown in Fig. 14 as a function of $M_{\tau'}$.

For the modified singlet VLL model with BR$(\tau' \to Z\tau) = 1$, the more optimistic results for visible cross sections after cuts for the $\geq 3e/\mu + 2\tau_h$, $\geq 4e/\mu + 1\tau_h$ and $\geq 5e/\mu$ inclusive signal regions are presented in Table XV. The predicted luminosities required for 95% C.L. exclusion with $Z_{\rm exc} \geq 1.645$ and $Z_{\rm disc} \geq 5$ discovery are shown in Fig. 15 for these three channels at $\sqrt{s} = 13$ TeV. In addition, Fig. 16 shows the results for the combined 5-lepton signal region obtained by summing these three channels. With an integrated luminosity of 100 fb^{-1}, a 95% C.L. exclusion can be expected in the combined 5-lepton search up to about $M_{\tau'} = 250$ GeV, even with a 50% fractional uncertainty in the background. The best of the individual channels for this search is $\geq 4e/\mu + 1\tau_h$. A potential $Z_{\rm disc} > 5$ discovery would require more than 100 fb^{-1} in this most optimistic case of BR$(\tau' \to Z\tau) = 1$, even for $M_{\tau'}$ less than 150 GeV, and even after combining the three individual 5-lepton channels, and discovering $M_{\tau'} = 200$ GeV would require 350 fb^{-1}. The discovery potential degrades completely for the $\Delta_b = 0.5b$ case.

TABLE XV. Signal and total background cross sections in the $\geq 4e/\mu + 1\tau_h$, $\geq 3e/\mu + 2\tau_h$ and $\geq 5e/\mu$ channels after inclusive selections, for the modified singlet VLL model with BR$(\tau' \to Z\tau) = 1$, at $\sqrt{s} = 13$ TeV.

$M_{\tau'}$ (GeV)	σ_s (fb) in $\geq 4e/\mu + 1\tau_h$	σ_s (fb) in $\geq 3e/\mu + 2\tau_h$	σ_s (fb) in $\geq 5e/\mu$
120	0.0453	0.0113	0.0297
130	0.0520	0.0149	0.0325
140	0.0505	0.0144	0.0355
150	0.0462	0.0138	0.0357
160	0.0418	0.0120	0.0338
180	0.0351	0.0110	0.0291
200	0.0261	0.0086	0.0224
250	0.0144	0.0044	0.0138
300	0.0079	0.0024	0.0080
Total background	0.0055	0.0065	0.0053

VII. OUTLOOK

In this paper we have studied possibilities for discovering or excluding vectorlike leptons at the LHC in different multilepton searches. We mainly looked at two different cases, the singlet VLL model and doublet VLL model, with small mixing allowing decays of vectorlike leptons to tau leptons, as described in the Introduction. (A previous paper [40] had already considered the more optimistic case of decays to muons.) We pointed out that there is an opportunity to set limits on vectorlike lepton production in the doublet VLL model using existing LHC data at $\sqrt{s} = 8$ TeV. This could be done with searches similar to the Run 1 ATLAS 3-lepton and 4-lepton searches [64,65] based on $\int L\,dt = 20.3$ fb^{-1}. In the 3-lepton channels, we found that our estimates for the visible signal cross section exceeds the ATLAS limit up to about $M_{\tau'} = 200$ GeV for both $\geq 3e/\mu$ and $2e/\mu + \geq 1\tau_h$ searches with off-Z and no-OSSF selections. While looking at the 4-lepton channels we again found that up to about $M_{\tau'} = 200$ GeV, our estimates for the visible cross section exceeds the ATLAS limit in two searches, $\geq 4e/\mu$ on-Z and $3e/\mu + \geq 1\tau_h$ no-Z.

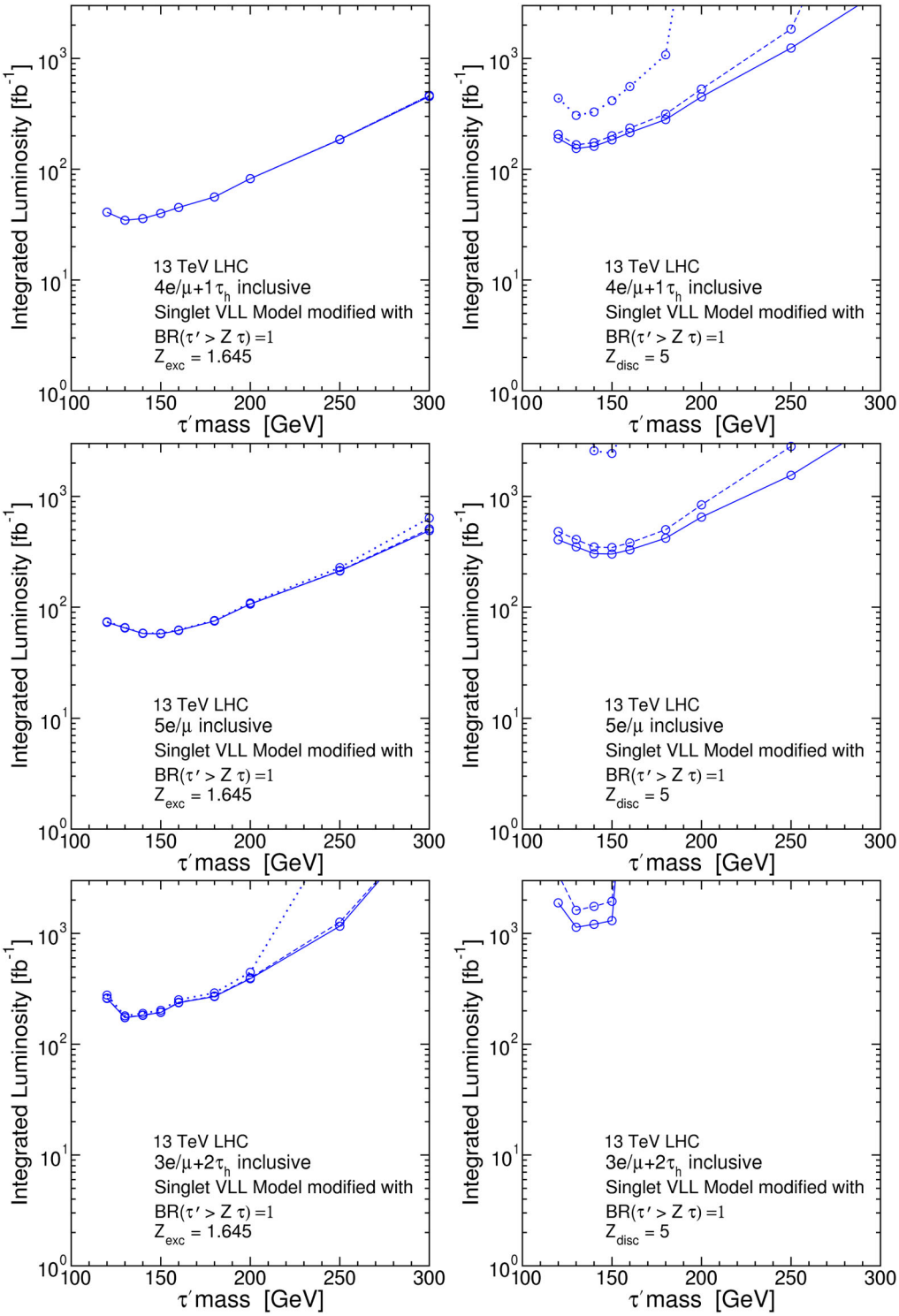

FIG. 15 (color online). Integrated luminosities needed for $Z_{\rm exc} = 1.645$ (95% C.L.) exclusion (left) or $Z_{\rm disc} = 5$ discovery (right), in the $\geq 4e/\mu + 1\tau_h$, $\geq 5e/\mu$ and $\geq 3e/\mu + 2\tau_h$ inclusive channels (from top to bottom), for the singlet VLL model with $\mathrm{BR}(\tau' \to Z\tau) = 1$, as a function of $M_{\tau'}$, at $\sqrt{s} = 13$ TeV, based on the results from Table XV. The different lines in each plot correspond to assumed background uncertainties $\Delta_b = 0.1b$ (solid), $\Delta_b = 0.2b$ (dashed), and $\Delta_b = 0.5b$ (dotted).

We then presented a simpler 4-lepton search strategy more appropriate for the the doublet VLL model. We came up with a different set of selections that we followed throughout the rest of the paper. Imposing a b-jet veto became very useful to reduce some of the background cross sections involving top quarks. We also used a set of equations as mentioned in the Introduction to calculate median expected significances for exclusion ($Z_{\rm exc}$). We

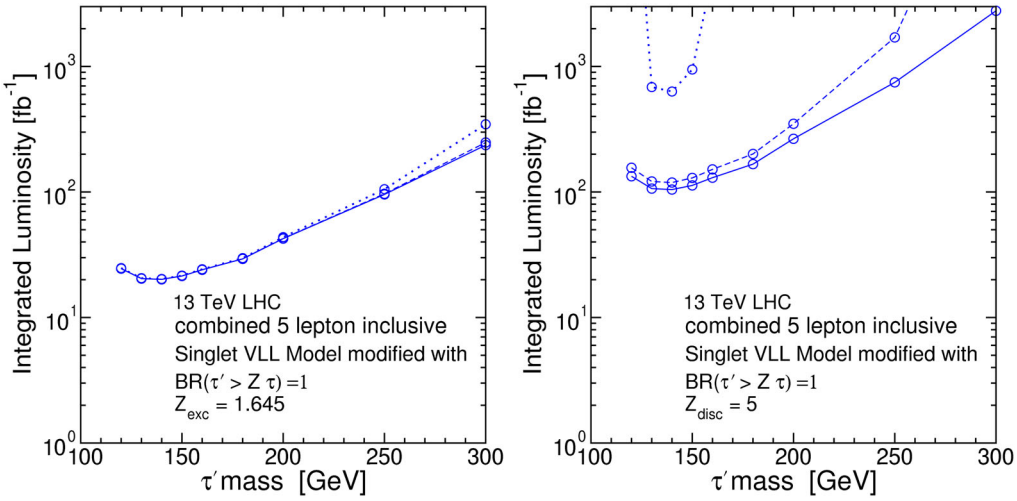

FIG. 16 (color online). Integrated luminosities needed for $Z_{\rm exc} = 1.645$ (95% C.L.) exclusion (left) or $Z_{\rm disc} = 5$ discovery (right) in the combined 5-lepton inclusive channel, for the modified singlet VLL model with $\mathrm{BR}(\tau' \to Z\tau) = 1$, as a function of $M_{\tau'}$, at $\sqrt{s} = 13$ TeV, based on the results from Table XV. The different lines in each plot correspond to assumed background uncertainties $\Delta_b = 0.1b$ (solid), $\Delta_b = 0.2b$ (dashed), and $\Delta_b = 0.5b$ (dotted).

found that the highest exclusion significance can be reached with the $\geq 3e/\mu + 1\tau_h$ channel, and $M_{\tau'}$ masses up to about 275 GeV could be excluded with 95% C.L. in both inclusive and no-Z searches with 20 fb^{-1} at $\sqrt{s} = 8$ TeV, provided that there is indeed no signal present.

We also studied the future prospects for vectorlike leptons at $\sqrt{s} = 13$ TeV. In the doublet VLL model, we estimated the integrated luminosities needed to set 95% C.L. exclusion and discovery with $Z_{\rm disc} \geq 5$ in 4-lepton and 5-lepton channels as a function of $M_{\tau'} = M_{\nu'}$. We find that it should be possible to set an exclusion up to $M_{\tau'} = 440$ GeV with 100 fb^{-1} of integrated luminosity, using several different 4-lepton channels with no-Z selections, even assuming 20% fractional uncertainty in the background. Discovery is possible with 100 fb^{-1} for $M_{\tau'}$ up to about 300 GeV using the same channels. In 5-lepton searches we found the inclusive search to do much better than the no-Z channels, because of the statistics-limited nature of the signal. The 5-lepton searches have the advantage of extremely small backgrounds. With inclusive 5-lepton searches we found that there is a chance to discover the vectorlike leptons in the doublet VLL model up to $M_{\tau'} = 250$ GeV with integrated luminosity of 100 fb^{-1}, even with 50% fractional uncertainties assumed for the backgrounds.

The singlet VLL model is much more difficult. We find that even setting a 95% C.L. exclusion is not possible with 4-lepton searches unless the background is known with less than 10% uncertainty. Even in the optimistic scenario that the background is known exactly, we find no expected exclusions with less than 350 fb^{-1}, and it would take 1000 fb^{-1} to exclude up to $M_{\tau'} = 200$ GeV. Using 5-lepton searches, excluding any range of masses for the singlet VLL model requires on the order of 1000 fb^{-1} of integrated luminosity.

We also considered a modified singlet VLL model, obtained by (arbitrarily) setting $\mathrm{BR}(\tau' \to Z\tau) = 1$, while assuming the same production cross section. While we did not specify a model exhibiting these characteristics, it is at least consistent in the sense that the Lagrangian terms governing production are distinct from the mixing terms governing the decays. Here, the 5-lepton signal seem to be the best, with 100 fb^{-1} providing an expected exclusion up to $M_{\tau'} = 250$ GeV, while discovery up to $M_{\tau'} = 200$ GeV would required 350 fb^{-1}.

In this paper, we have only looked at signals based on relatively clean multilepton final states, including up to 2 hadronic taus. There are other channels which can be looked at, including those with more than 2 b-jets from Higgs and Z decays. For example, these could include the channel $4b + 2\tau_h$, for which physics backgrounds should be small, but detector backgrounds are harder to estimate.

We note that the projections made in this paper are heavily dependent on our simulation tools, and only the experimental collaborations can provide real exclusions (or discovery), based on background estimates driven and verified by data and knowledge of detector responses. However, we believe that it is clear that the opportunity to conduct searches for vectorlike leptons that decay to taus should be pursued at the LHC.

ACKNOWLEDGMENTS

We thank Jahred Adelman and Glen Cowan for helpful discussions about the treatment of significances in the presence of background uncertainties. This work was supported in part by the National Science Foundation Grant No. PHY-1417028.

[1] T. Moroi and Y. Okada, Radiative corrections to Higgs masses in the supersymmetric model with an extra family and antifamily, Mod. Phys. Lett. A **07**, 187 (1992).

[2] T. Moroi and Y. Okada, Upper bound of the lightest neutral Higgs mass in extended supersymmetric Standard Models, Phys. Lett. B **295**, 73 (1992).

[3] K. S. Babu, I. Gogoladze, and C. Kolda, Perturbative unification and Higgs boson mass bounds, arXiv:hep-ph/0410085.

[4] K. S. Babu, I. Gogoladze, M. U. Rehman, and Q. Shafi, Higgs Boson mass, sparticle spectrum and little Hierarchy problem in extended MSSM, Phys. Rev. D **78**, 055017 (2008).

[5] S. P. Martin, Extra vectorlike matter and the lightest Higgs scalar boson mass in low-energy supersymmetry, Phys. Rev. D **81**, 035004 (2010).

[6] P. W. Graham, A. Ismail, S. Rajendran, and P. Saraswat, A little solution to the little Hierarchy problem: A vectorlike generation, Phys. Rev. D **81**, 055016 (2010).

[7] S. P. Martin, Raising the Higgs mass with Yukawa couplings for isotriplets in vectorlike extensions of minimal supersymmetry, Phys. Rev. D **82**, 055019 (2010).

[8] M. Endo, K. Hamaguchi, S. Iwamoto, and N. Yokozaki, Higgs mass and muon anomalous magnetic moment in supersymmetric models with vectorlike matters, Phys. Rev. D **84**, 075017 (2011).

[9] J. L. Evans, M. Ibe, and T. T. Yanagida, Probing extra matter in gauge mediation through the lightest Higgs boson mass, arXiv:1108.3437.

[10] T. Li, J. A. Maxin, D. V. Nanopoulos, and J. W. Walker, A Higgs mass shift to 125 GeV and a multijet supersymmetry signal: Miracle of the flippons at the $\sqrt{s} = 7$ TeV LHC, Phys. Lett. B **710**, 207 (2012).

[11] T. Moroi, R. Sato, and T. T. Yanagida, Extra matters decree the relatively heavy Higgs of mass about 125 GeV in the supersymmetric model, Phys. Lett. B **709**, 218 (2012).

[12] M. Endo, K. Hamaguchi, S. Iwamoto, and N. Yokozaki, Higgs mass, muon g-2, and LHC prospects in gauge mediation models with vectorlike matters, Phys. Rev. D **85**, 095012 (2012).

[13] M. Endo, K. Hamaguchi, S. Iwamoto, and N. Yokozaki, Vacuum stability bound on extended GMSB models, J. High Energy Phys. 06 (2012) 060.

[14] K. Nakayama and N. Yokozaki, Peccei-Quinn extended gauge-mediation model with vector-like matter, J. High Energy Phys. 11 (2012) 158.

[15] S. P. Martin and J. D. Wells, Implications of gauge-mediated supersymmetry breaking with vector-like quarks and a 125 GeV Higgs boson, Phys. Rev. D **86**, 035017 (2012).

[16] S. Dimopoulos, N. Tetradis, R. Esmailzadeh, and L. J. Hall, TeV dark matter, Nucl. Phys. **B349**, 714 (1991); S. Dimopoulos, N. Tetradis, R. Esmailzadeh, and L. J. Hall, Erratum, Nucl. Phys. **B357**, 308 (1991).

[17] M. Sher, Charged leptons with nanosecond lifetimes, Phys. Rev. D **52**, 3136 (1995).

[18] S. D. Thomas and J. D. Wells, Phenomenology of Massive Vectorlike Doublet Leptons, Phys. Rev. Lett. **81**, 34 (1998).

[19] P. H. Frampton, P. Q. Hung, and M. Sher, Quarks and leptons beyond the third generation, Phys. Rep. **330**, 263 (2000).

[20] F. del Aguila, A. Carmona, and J. Santiago, Neutrino masses from an A4 symmetry in holographic composite Higgs models, J. High Energy Phys. 08 (2010) 127; Tau custodian searches at the LHC, Phys. Lett. B **695**, 449 (2011); A. Carmona and F. Goertz, Custodial leptons and Higgs decays, J. High Energy Phys. 04 (2013) 163.

[21] R. Dermisek, Insensitive unification of gauge couplings, Phys. Lett. B **713**, 469 (2012).

[22] A. Joglekar, P. Schwaller, and C. E. M. Wagner, Dark matter and enhanced Higgs to di-photon rate from vector-like leptons, J. High Energy Phys. 12 (2012) 064.

[23] J. Kearney, A. Pierce, and N. Weiner, Vectorlike fermions and Higgs couplings, Phys. Rev. D **86**, 113005 (2012).

[24] J. Halverson, N. Orlofsky, and A. Pierce, Vectorlike leptons as the tip of the dark matter iceberg, Phys. Rev. D **90**, 015002 (2014).

[25] C. Arina, R. N. Mohapatra, and N. Sahu, Co-genesis of matter and dark matter with vector-like fourth generation leptons, Phys. Lett. B **720**, 130 (2013).

[26] B. Batell, S. Jung, and H. M. Lee, Singlet assisted vacuum stability and the Higgs to diphoton rate, J. High Energy Phys. 01 (2013) 135.

[27] R. Dermisek, Unification of gauge couplings in the standard model with extra vectorlike families, Phys. Rev. D **87**, 055008 (2013).

[28] P. Schwaller, T. M. P. Tait, and R. Vega-Morales, Dark matter and vectorlike leptons from gauged lepton number, Phys. Rev. D **88**, 035001 (2013).

[29] R. Dermisek and A. Raval, Explanation of the muon g-2 anomaly with vectorlike leptons and its implications for Higgs decays, Phys. Rev. D **88**, 013017 (2013).

[30] M. Fairbairn and P. Grothaus, Baryogenesis and dark matter with vector-like fermions, J. High Energy Phys. 10 (2013) 176.

[31] K. Ishiwata and M. B. Wise, Phenomenology of heavy vectorlike leptons, Phys. Rev. D **88**, 055009 (2013).

[32] W. Altmannshofer, M. Bauer, and M. Carena, Exotic leptons: Higgs, flavor and collider phenomenology, J. High Energy Phys. 01 (2014) 060.

[33] A. Falkowski, D. M. Straub, and A. Vicente, Vector-like leptons: Higgs decays and collider phenomenology, J. High Energy Phys. 05 (2014) 092.

[34] B. A. Dobrescu and C. Frugiuele, Hidden GeV-Scale Interactions of Quarks, Phys. Rev. Lett. **113**, 061801 (2014).

[35] S. A. R. Ellis, R. M. Godbole, S. Gopalakrishna, and J. D. Wells, Survey of vector-like fermion extensions of the standard model and their phenomenological implications, J. High Energy Phys. 09 (2014) 130.

[36] A. Falkowski and R. Vega-Morales, Exotic Higgs decays in the golden channel, J. High Energy Phys. 12 (2014) 037.

[37] B. Holdom and M. Ratzlaff, Neglected heavy leptons at the LHC, Phys. Rev. D **90**, 013015 (2014).

[38] R. Dermisek, A. Raval, and S. Shin, Effects of vectorlike leptons on $h \to 4\ell$ and the connection to the muon g-2 anomaly, Phys. Rev. D **90**, 034023 (2014).

[39] B. A. Dobrescu and A. Martin, Interpretations of anomalous LHC events with electrons and jets, Phys. Rev. D **91**, 035019 (2015).

[40] R. Dermisek, J. P. Hall, E. Lunghi, and S. Shin, Limits on vectorlike leptons from searches for anomalous production of multilepton events, J. High Energy Phys. 12 (2014) 013.
[41] B. Holdom and M. Ratzlaff, Distinctive heavy Higgs boson decays, Phys. Rev. D **91**, 035031 (2015).
[42] K. Ishiwata, Z. Ligeti, and M. B. Wise, New vector-like fermions and flavor physics, J. High Energy Phys. 10 (2015) 027.
[43] N. Bizot and M. Frigerio, Fermionic extensions of the standard model in light of the Higgs couplings, arXiv: 1508.01645.
[44] R. Dermisek, E. Lunghi, and S. Shin, Two Higgs doublet model with vectorlike leptons and contributions to $pp \to WW$ and $H \to WW$, arXiv:1509.04292.
[45] S. Bhattacharya, N. Sahoo, and N. Sahu, Minimal vectorlike leptonic dark matter and signatures at the LHC, arXiv:1510.02760.
[46] S. Fichet, G. von Gersdorff, O. Kepka, B. Lenzi, C. Royon, and M. Saimpert, Probing new physics in diphoton production with proton tagging at the Large Hadron Collider, Phys. Rev. D **89**, 114004 (2014); S. Fichet, G. von Gersdorff, B. Lenzi, C. Royon, and M. Saimpert, Light-by-light scattering with intact protons at the LHC: From standard model to new physics, J. High Energy Phys. 02 (2015) 165.
[47] H. K. Dreiner, H. E. Haber., and S. P. Martin, Two-component spinor techniques and Feynman rules for quantum field theory and supersymmetry, Phys. Rep. **494**, 1 (2010).
[48] S. P. Martin, TASI 2011 lectures notes: Two-component fermion notation and supersymmetry, arXiv:1205.4076.
[49] G. Cowan, Two developments in tests for discovery: Use of weighted Monte Carlo events and an improved measure, Progress on Statistical Issues in Searches, SLAC, 2012 (unpublished).
[50] G. Cowan, K. Cranmer, E. Gross, and O. Vitells, Asymptotic formulae for likelihood-based tests of new physics, Eur. Phys. J. C **71**, 1554 (2011); G. Cowan, K. Cranmer, E. Gross, and O. Vitells, Erratum, Eur. Phys. J. C **73**, 2501 (2013).
[51] T.-P. Li and Y.-Q. Ma, Analysis methods for results in gamma-ray astronomy, Astrophys. J. **272**, 317 (1983).
[52] R. D. Cousins, J. T. Linnemann, and J. Tucker, Evaluation of three methods for calculating statistical significance when incorporating a systematic uncertainty into a test of the background-only hypothesis for a Poisson process, Nucl. Instrum. Methods Phys. Res., Sect. A **595**, 480 (2008).
[53] J. Alwall, M. Herquet, F. Maltoni, O. Mattelaer, and T. Stelzer, MadGraph 5: Going beyond, J. High Energy Phys. 06 (2011) 128.
[54] A. Alloul, N. D. Christensen, C. Degrande, C. Duhr, and B. Fuks, FeynRules 2.0—A complete toolbox for tree-level phenomenology, Comput. Phys. Commun. **185**, 2250 (2014).
[55] T. Sjostrand, S. Mrenna, and P. Z. Skands, PYTHIA 6.4 physics and manual, J. High Energy Phys. 05 (2006) 026.
[56] J. de Favereau, C. Delaere, P. Demin, A. Giammanco, V. Lematre, A. Mertens, and M. Selvaggi, DELPHES 3, A modular framework for fast simulation of a generic collider experiment, J. High Energy Phys. 02 (2014) 057.
[57] J. M. Campbell and R. K. Ellis, An Update on vector boson pair production at hadron colliders, Phys. Rev. D **60**, 113006 (1999).
[58] F. Campanario, V. Hankele, C. Oleari, S. Prestel, and D. Zeppenfeld, QCD corrections to charged triple vector boson production with leptonic decay, Phys. Rev. D **78**, 094012 (2008).
[59] M. V. Garzelli, A. Kardos, C. G. Papadopoulos, and Z. Trocsanyi, $t\bar{t}$ W^{+-} and $t\bar{t}Z$ hadroproduction at NLO accuracy in QCD with parton shower and hadronization effects, J. High Energy Phys. 11 (2012) 056.
[60] S. Heinemeyer *et al.* (LHC Higgs Cross Section Working Group Collaboration), Handbook of LHC Higgs cross sections: 3. Higgs properties, arXiv:1307.1347.
[61] N. Chen, C. Du, Y. Fang, and L. C. Lu, LHC searches for the heavy Higgs boson via two B jets plus diphoton, Phys. Rev. D **89**, 115006 (2014).
[62] A. Djouadi, J. Kalinowski, and M. Spira, HDECAY: A program for Higgs boson decays in the Standard Model and its supersymmetric extension, Comput. Phys. Commun. **108**, 56 (1998).
[63] R. Ruiz, QCD Corrections to pair production of type III seesaw leptons at hadron colliders, arXiv:1509.05416.
[64] G. Aad *et al.* (ATLAS Collaboration), Search for new phenomena in events with three or more charged leptons in pp collisions at $\sqrt{s} = 8$ TeV with the ATLAS detector, J. High Energy Phys. 08 (2015) 138.
[65] G. Aad *et al.* (ATLAS Collaboration), Search for supersymmetry in events with four or more leptons in $\sqrt{s} =$ 8 TeV pp collisions with the ATLAS detector, Phys. Rev. D **90**, 052001 (2014).